J. Fluid Mech. (2009), *vol.* 624, *pp.* 293–337.
doi:10.1017/S0022112008005417 Printed in the United Kingdom

Small-deformation theory for a surfactant-covered drop in linear flows

PETIA M. VLAHOVSKA[1]†, JERZY BŁAWZDZIEWICZ[2] AND MICHAEL LOEWENBERG[3]

[1]Thayer School of Engineering, Dartmouth College, Hanover, NH 03755, USA

[2]Department of Mechanical Engineering, Yale University, New Haven, CT 06520-8284, USA

[3]Department of Chemical Engineering, Yale University, New Haven, CT 06520-8286, USA

(Received 7 May 2008 and in revised form 27 November 2008)

A small-deformation perturbation analysis is developed to study the effect of surfactant on drop dynamics in viscous flows. The surfactant is assumed to be insoluble in the bulk-phase fluids; the viscosity ratio and surfactant elasticity parameters are arbitrary. Under small-deformation conditions, the drop dynamics are described by a system of ordinary differential equations; the governing equations are given explicitly for the case of axisymmetric and two-dimensional imposed flows. Analytical results accurate to third order in the flow-strength parameter (capillary number) are derived (i) for the stationary drop shape and surfactant distribution in simple shear and axisymmetric straining flows, and (ii) for the rheology of a dilute emulsion in shear flow which include a shear-thinning viscosity and non-zero normal stresses. For drops with clean interfaces, the small-deformation theory presented here improves the results of Barthès-Biesel & Acrivos (*J. Fluid Mech.*, vol. 61, 1973, p. 1). Boundary integral simulations are used to test our theory and explore large-deformation conditions.

1. Introduction

Surface active agents (e.g. surfactants, compatibilizers, and proteins) are often employed to control properties of emulsions and polymer blends; they are added to stabilize the emulsions, to facilitate drop breakup, to prevent drop coalescence, etc. (Lequeux 1998; Van Puyvelde, Velankar & Moldenaers 2001; Tucker & Moldenaers 2002; Fischer & Erni 2007). Quantitative understanding of the effect of surfactants on drop dynamics represents a challenging problem because drop shape and surfactant distribution at the interface are not given *a priori* but are determined by the balance between interfacial and fluid stresses.

In the absence of surfactants, drop deformation is governed solely by the isotropic surface tension, which acts to keep the drop spherical (Rallison 1984; Stone 1994). In the presence of surfactants, surface tension is reduced and may become non-uniform. Experimental studies have revealed an intricate interplay between shape deformation, surfactant redistribution on drop interface and bulk flows (Stone & Leal 1990; Velankar *et al.* 2001; Hu & Lips 2003; Jeon & Macosko 2003; Velankar *et al.* 2004*a*, *b*). For example, in linear flows (see figure 1), fluid motion elongates the drop and sweeps the surfactant towards the drop ends. The accumulation of surfactant at the tips decreases the surface tension. As a result, the curvature increases as needed

† Email address for correspondence: petia.vlahovska@dartmouth.edu

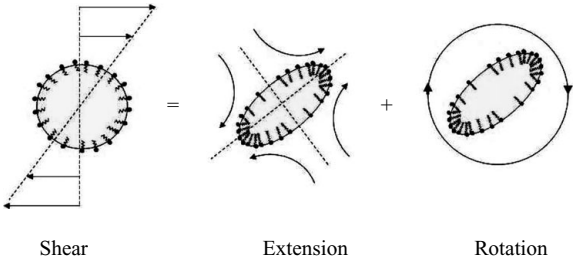

FIGURE 1. Illustration of a surfactant-covered drop in a simple-shear flow.

to maintain the normal stress balance. The increase of interfacial area accompanying drop deformation leads to dilution of overall surfactant concentration and increase of surface tension. The non-uniform surfactant distribution gives rise to gradients of the surface tension (Marangoni stresses). Tip-stretching, dilution and Marangoni stresses have been studied extensively for axisymmetric flows and two-dimensional drops, mainly by means of numerical simulations (Stone & Leal 1990; Milliken, Stone & Leal 1993; Eggleton, Pawar & Stebe 1998; Eggleton, Tsai & Stebe 2001; James & Lowengrub 2004; Lee & Pozrikidis 2006; Xu *et al.* 2006; Muradoglu & Tryggvason 2008), although recently analytical results for a highly deformed bubble have been obtained using slender-body theory (Booty & Siegel 2005).

In shear flows, the rotational flow component rotates the drop away from the extensional axis and continuously redistributes the surfactant, thereby decreasing the non-uniformities and shape distortion. The effect of rotation becomes increasingly important as the viscosity contrast increases. Three-dimensional simulations have been developed to explore the dynamics of surfactant-covered drops in shear flows (Li & Pozrikidis 1997; Yon & Pozrikidis 1998; Bazhlekov, Anderson & Meijer 2004; Pozrikidis 2004; Vlahovska, Bławzdziewicz & Loewenberg 2005; Bazhlekov, Anderson & Meijer 2006; Feigl *et al.* 2007). However, with exception of Bazhlekov *et al.* (2006), these studies are limited to equiviscous drop and suspending fluids because simulations of high-viscosity drops are computationally expensive.

Since high-viscosity drops deform little in shear flow, analytical theories based on perturbation analyses for small deviations from sphericity provide an attractive alternative to the costly numerical simulations. Most work has been focused on surfactant-free drops, where expansions for up to third order in shape deformation have been derived (Taylor 1934; Cox 1969; Frankel & Acrivos 1970; Barthès-Biesel & Acrivos 1973*a*; Greco 2002). Rallison (1980) provides a clear summary of the expansions based on different small parameters (e.g. capillary number, viscosity ratio).

Similar analyses of surfactant-covered drops are at an earlier stage. A leading-order perturbation theory, which includes surface shear and dilatational viscosities as well as mass transfer from the bulk was developed by Flumerfelt (1980). Stone & Leal (1990) also considered the near-sphere limit analytically and included surface diffusion in their analysis. These theories describe the drop deformation to leading order but are insufficient for predicting the non-Newtonian emulsion rheology. A solution beyond the leading linear order is a difficult task because it requires evaluation of boundary conditions, e.g. matching inner and outer velocities or stresses, on the interface of the deformed drop. This problem can be circumvented for the special case of a drop with the same viscosity as the suspending fluid. For this problem, the fluid velocity field can be computed directly from the interfacial stresses using the integral representation of the Stokes flow solution (Kim & Karrila 1991; Pozrikidis 1992). We have developed

a third-order perturbation solution for the equiviscous drop (Vlahovska *et al.* 2005) and derived explicit results for the stationary drop shape, surfactant distribution and effective stresses of a dilute emulsion of deformable surfactant-covered drops.

The present work addresses the general case of a drop with arbitrary viscosity contrast. In order to derive an analytical solution for small drop deformation, we develop a perturbation formalism capable of treating the matching process at the deformed interface. The paper is organized as follows. Section 2 presents the formulation of the problem, while § 3 outlines the general idea of the perturbation solution. Section 4 provides details of the solution; a reader more interested in the applications may skip this rather technical part. Section 5 presents the second-order evolution equations for the shape and surfactant distribution in linear flows as well as the effective stress of a dilute emulsion. Sections 6 and 7 provide the weak-flow expansions for the stationary shape, surfactant distribution and emulsion effective stresses for two common types of flow: axisymmetric extensional and a simple-shear flows; we compare the results from our third-order small-deformation theory with boundary integral simulations. The combined analytical and numerical study leads to an improved quantitative description of the effects of surfactant on drop dynamics. In § 8, we give the complete third-order shape-evolution equations for a surfactant-free drop, and we present the relation between our analysis and that of Barthès-Biesel & Acrivos (1973*a*).

2. Problem statement

Consider an initially spherical, neutrally buoyant drop with equilibrium radius a and viscosity η^{in} suspended in an unbounded fluid with viscosity η^{out}. A monolayer of insoluble surfactant is adsorbed on the drop interface. At rest, the surfactant distribution is uniform and the equilibrium surfactant concentration is Γ_{eq}; the corresponding interfacial tension is σ_{eq}. The coordinate system employed is spherical (r, θ, ϕ), with the origin coinciding with the centre of mass of the drop. The drop is placed in a linear flow

$$\boldsymbol{u}^{\infty}(\boldsymbol{r}) = \dot{\gamma}\boldsymbol{E}\cdot\boldsymbol{r}, \tag{2.1}$$

where $\dot{\gamma}$ is the strain rate. $\boldsymbol{E}$ is a traceless constant tensor, which characterizes the velocity gradient

$$\boldsymbol{E} = \tfrac{1}{2}\begin{pmatrix} 0 & 1+\beta & 0 \\ 1-\beta & 0 & 0 \\ 0 & 0 & 0 \end{pmatrix} \tag{2.2}$$

and β is the rotational component of the flow. Simple-shear flow is given by $\beta = 1$.

Hereafter, the surfactant concentration is normalized by Γ_{eq}; all other quantities are rescaled using η^{out}, a and $\dot{\gamma}$. Accordingly, the timescale is $\dot{\gamma}^{-1}$, the velocity scale is $\dot{\gamma}a$, bulk viscous stresses are scaled with $\eta^{out}\dot{\gamma}$ and the scale for interfacial tension is σ_{eq}.

2.1. *Governing equations*

In the creeping flow limit, the fluid motion inside and outside the drop obeys the Stokes equations

$$\nabla\cdot\boldsymbol{T} = 0, \qquad \nabla\cdot\boldsymbol{u} = 0, \tag{2.3}$$

where the bulk hydrodynamic stresses are

$$\boldsymbol{T}^{out} = -p^{out}\boldsymbol{I} + [\nabla\boldsymbol{u}^{out} + (\nabla\boldsymbol{u}^{out})^{T}], \tag{2.4a}$$

$$\boldsymbol{T}^{in} = -p^{in}\boldsymbol{I} + (\chi - 1)[\nabla \boldsymbol{u}^{in} + (\nabla \boldsymbol{u}^{in})^T], \tag{2.4b}$$

$\boldsymbol{u}$ denotes the velocity and p is the pressure.

The viscosity contrast is characterized by

$$\chi = 1 + \frac{\eta^{in}}{\eta^{out}}. \tag{2.5}$$

Since this parameter is always greater than unity, its inverse is well defined. Thus, it can serve as a small parameter for a perturbation analysis of highly viscous drops. In the case of a spherical surfactant-covered drop, χ^{-1} provided expansion that was converging much faster than the one based on the usual inverse viscosity ratio η^{out}/η^{in} (Bławzdziewicz, Vlahovska & Loewenberg 2000).

Far from the drop, the flow tends to the undisturbed external flow,

$$\boldsymbol{u}^{out} \to \boldsymbol{u}^{\infty} \quad \text{as} \quad \boldsymbol{r} \to \infty. \tag{2.6}$$

Fluid velocity is continuous across the drop interface

$$\boldsymbol{u}^{out} = \boldsymbol{u}^{in} \quad \text{at} \quad r = r_s, \tag{2.7}$$

where r_s denotes the position of the interface. Drop interface moves with the fluid velocity, i.e.

$$\frac{\partial H}{\partial t} + \boldsymbol{u} \cdot \nabla H = 0 \quad r = r_s, \tag{2.8}$$

where $H = r - r_s$ represents the interface as the set of points $\boldsymbol{r}$, where $H(\boldsymbol{r}, t) \equiv 0$. The shape function H defines the outward pointing unit normal to the drop interface

$$\boldsymbol{n} = \frac{\nabla H}{|\nabla H|}. \tag{2.9}$$

The evolution of the distribution of an insoluble, non-diffusing surfactant is governed by a time-dependent convective (Stone 1990; Wong, Rumschitzki & Maldarelli 1996)

$$\frac{\partial \Gamma}{\partial t} + \nabla_s \cdot (\boldsymbol{u}_s \Gamma) + \Gamma(\boldsymbol{u} \cdot \boldsymbol{n})\nabla_s \cdot \boldsymbol{n} = 0 \quad \text{at} \quad r = r_s, \tag{2.10}$$

where ∇_s is the surface gradient operator, $\nabla_s = (\boldsymbol{I} - \boldsymbol{nn}) \cdot \nabla$.

The jump of the hydrodynamic tractions across the drop interface is balanced by the interfacial stresses

$$\boldsymbol{n} \cdot \boldsymbol{T}^{out} - \boldsymbol{n} \cdot \boldsymbol{T}^{in} = \boldsymbol{t}. \tag{2.11}$$

Interfacial stresses arise from non-uniform curvature and gradients in surface tension

$$\boldsymbol{t} = Ca^{-1}(\sigma \boldsymbol{n} \nabla_s \cdot \boldsymbol{n}) - Ma \nabla_s \sigma, \tag{2.12}$$

where $\nabla_s \cdot \boldsymbol{n}$ is the local mean curvature. The capillary number, defined as

$$Ca = \frac{\eta^{out} a \dot{\gamma}}{\sigma_{eq}}, \tag{2.13}$$

reflects the relative strength of the distorting viscous and restoring surface-tension forces. Likewise,

$$Ma^{-1} = \frac{\eta^{out} a \dot{\gamma}}{\Delta \sigma}, \tag{2.14}$$

reflects the relative strength of the distorting viscous and restoring Marangoni stresses.

$$\Delta\sigma = -\Gamma_{eq}\left(\frac{\partial\sigma}{\partial\Gamma}\right)_{\Gamma=\Gamma_{eq}}$$

is the characteristic magnitude of the surface-tension variations that result from perturbations of the local surfactant concentration Γ about the equilibrium value Γ_{eq}.

The dependence of the surface tension on the local surfactant concentration is generally nonlinear (Pawar & Stebe 1996; Eggleton *et al.* 1998). However, for small perturbations around equilibrium or dilute concentrations, the equation of state can be linearized

$$\sigma(\Gamma) = 1 - E(\Gamma - 1). \tag{2.15}$$

The elasticity number is given by

$$E = \frac{\Delta\sigma}{\sigma_{eq}} = CaMa. \tag{2.16}$$

In this study, we choose Ca as the dimensionless strain rate to define the flow. The elasticity, E, and the viscosity contrast, χ, are flow-independent material parameters characterizing the surfactant monolayer and the fluids. Our previous work focused on the effect of surfactant elasticity at fixed viscosity contrast (Vlahovska *et al.* 2005). In this paper, we explore the effects of the viscosity contrast at a given surfactant elasticity.

2.2. *Effective rheological properties*

In the linear flow (2.1), the effective stress of a dilute emulsion with volume fraction ϕ is given by

$$\Sigma = 2\boldsymbol{E}^s + \phi\boldsymbol{T}^d, \tag{2.17}$$

where $\boldsymbol{E}^s$ denotes the symmetric part of the velocity gradient tensor (2.2) and $\boldsymbol{T}^d$ is the drop contribution. The emulsion shear rheology is fully characterized by the shear viscosity Σ_{xy} and normal stress differences $N_1 = \boldsymbol{T}^d_{xx} - \boldsymbol{T}^d_{yy}$ and $N_2 = \boldsymbol{T}^d_{yy} - \boldsymbol{T}^d_{xx}$.

The zero-shear rate limit of the viscosity of a dilute emulsion of surfactant-covered drops is given by Einstein's result for suspension of hard spheres, $\boldsymbol{T}^d_{12} = 5/2$ (Bławzdziewicz *et al.* 2000). At finite shear rates, drop deformation and Marangoni stresses give rise to shear thinning and normal stresses.

3. Small-deformation analysis

In a reference frame with the drop centre at $r = 0$, the position of the drop interface is specified by

$$r_s = \alpha + f(\Omega), \tag{3.1}$$

where f is the deviation of the drop shape from a sphere, which depends only on the solid angle Ω and has a vanishing angular average

$$\int f\,\mathrm{d}\Omega = 0. \tag{3.2}$$

The isotropic contribution α is determined by the constraint for constant drop volume

$$\int(\alpha + f)^3\,\mathrm{d}\Omega = 4\pi. \tag{3.3}$$

The evolution of interface (2.8) in terms of the shape perturbation f becomes

$$\frac{\partial f}{\partial t} = \boldsymbol{u}\cdot(\hat{\boldsymbol{r}} - \nabla f) \quad r = r_s. \tag{3.4}$$

The evaluation of the surfactant conservation equation (2.10) on a deforming interface represents a complicated problem because of the surface divergence operator. However, if the surfactant distribution is projected onto a sphere, $\tilde{\Gamma} = \Gamma r_s^2/\boldsymbol{n}\cdot\hat{\boldsymbol{r}}$ (Vlahovska *et al.* 2005), the surfactant conservation simplifies because the surface divergence is evaluated on a sphere. Similar to (3.1), the projected surfactant distribution can be represented as

$$\tilde{\Gamma} = 1 + g, \tag{3.5}$$

where g denotes the local, flow-induced variation of surfactant concentration. Thus the evolution (2.10) takes the form

$$\frac{\partial g}{\partial t} = -\tilde{\nabla}\cdot[\tilde{\boldsymbol{u}}(1+g)], \tag{3.6}$$

where $\tilde{\boldsymbol{u}}$ is the tangential angular velocity

$$\tilde{\boldsymbol{u}} = r_s^{-1}(\boldsymbol{I} - \hat{\boldsymbol{r}}\hat{\boldsymbol{r}})\cdot\boldsymbol{u} \quad r = r_s. \tag{3.7}$$

For small deviations from equilibrium characterized by some relevant parameter ε we seek to obtain evolution equations for the shape (3.4) and the surfactant concentration (3.6) as third-order regular perturbation expansions in the small parameter ε

$$\frac{\partial f}{\partial t} = \sum_{p=0}^{3}\varepsilon^p F_p(f,g), \qquad \frac{\partial g}{\partial t} = \sum_{p=0}^{3}\varepsilon^p G_p(f,g). \tag{3.8}$$

In creeping flows and moderate viscosity ratios, drop shape remains close to spherical provided that the capillary number is small. In this work, we focus on this weak-flow limit, i.e. $\varepsilon = Ca$. If $E \sim O(1)$ surfactant distribution remains nearly uniform, and the perturbation in the surfactant concentration around its equilibrium distribution also scales as ε. In shear flows, high-viscosity contrast between the drop and suspending fluids limits the shape and surfactant distortion because of the increased rate of drop rotation. Thus, another choice for the small parameter is the viscosity contrast, χ^{-1}; the results of this analysis will be presented in a forthcoming paper.

The spherical geometry of the problem suggests to expand the position of drop interface and surfactant concentration in scalar spherical harmonics (A 1)

$$f = \sum_{j=2}^{\infty}\sum_{m=-j}^{j} f_{jm}Y_{jm}, \quad g = \sum_{j=2}^{\infty}\sum_{m=-j}^{j} g_{jm}Y_{jm}. \tag{3.9}$$

In the following section, we present details of our solution. The reader more interested in the final results than the technical details may proceed directly to § 5, where the evolution equations for the drop-shape deformation and emulsion-effective stress are listed.

4. Solution

4.1. *Evaluation of quantities at the deformed interface: general formalism*

Similar to the shape and surfactant concentration (3.9), all quantities are represented as perturbation expansions in the small parameter ε, e.g. the velocity and stress fields

are

$$\boldsymbol{u}(\boldsymbol{r}) = \sum_{p=0}^{3} \varepsilon^p \boldsymbol{u}_p(\boldsymbol{r}), \qquad \boldsymbol{T}(\boldsymbol{r}) = \sum_{p=0}^{3} \varepsilon^p \boldsymbol{T}_p(\boldsymbol{r}). \tag{4.1}$$

Solving the hydrodynamic problem requires evaluation of the boundary conditions for the velocity continuity (2.7) and stress balance (2.11) at the interface of the deformed drop. For small deviations of the drop shape from a sphere, all quantities that are to be evaluated at the deformed shape interface are approximated in terms of equivalent quantities on a sphere using a Taylor series expansion around $r = 1$ for $\varepsilon \ll 1$.

We first proceed to obtain the surface velocity. The combination of (4.1) with the Taylor series expansion for the velocity fields yields

$$\boldsymbol{u}(r = r_s) = \sum \varepsilon^p \bar{\boldsymbol{u}}_p(\Omega), \tag{4.2}$$

where

$$\bar{\boldsymbol{u}}_p(\Omega) = \sum_{n=0}^{p} \frac{f^n}{n!} \left. \frac{\mathrm{d}^n \boldsymbol{u}_{p-n}(r)}{\mathrm{d}\, r^n} \right|_{r=1}. \tag{4.3}$$

The continuity of velocity (2.7) must hold term by term

$$\bar{\boldsymbol{u}}_p^{in}(\Omega) = \bar{\boldsymbol{u}}_p^{out}(\Omega) + \boldsymbol{u}_p^{\infty}(\Omega), \tag{4.4}$$

where $\boldsymbol{u}_p^{\infty}(\Omega)$ denotes the Taylor series expansion of the external flow velocity (2.1). Note that for linear flows (2.1), $\boldsymbol{u}^{\infty}(\boldsymbol{r})$ is linear in r and, therefore, the terms $\boldsymbol{u}_p^{\infty}$ of order $p \geqslant 2$ vanish.

The hydrodynamic tractions at the deformed interface,

$$\boldsymbol{\tau}(\boldsymbol{r}_s) = \boldsymbol{n} \cdot \boldsymbol{T}(\boldsymbol{r}_s), \tag{4.5}$$

are expanded as

$$\boldsymbol{\tau}(\boldsymbol{r}_s) = \sum_{p=0}^{3} \varepsilon^p \boldsymbol{\tau}_p(\Omega). \tag{4.6}$$

The expansion terms

$$\boldsymbol{\tau}_p(\Omega) = \hat{\boldsymbol{r}} \cdot \bar{\boldsymbol{T}}_p + \sum_{k=1}^{p} \boldsymbol{n}_{p-k} \cdot \bar{\boldsymbol{T}}_k \tag{4.7}$$

are obtained by combining the normal vector expansion

$$\boldsymbol{n}(\Omega) = \hat{\boldsymbol{r}} + \sum_{p=1}^{3} \varepsilon^p \boldsymbol{n}_p(\Omega) \tag{4.8}$$

with the stresses expansion (4.1). $\bar{\boldsymbol{T}}_n(\Omega)$ denotes the nth term in the Taylor series for the stresses (defined analogously to the surface velocity (4.2), (4.3)). The stress jump condition (2.11) must hold at any perturbation order, hence

$$\boldsymbol{\tau}_p^{out}(\Omega) - (\chi - 1)\boldsymbol{\tau}_p^{in}(\Omega) = \boldsymbol{t}_p(\Omega), \tag{4.9}$$

where $\boldsymbol{t}_p$ is the corresponding term from the interfacial stress expansion

$$\boldsymbol{t} = \sum_{p=0}^{3} \varepsilon^p (Ca)^{-1} \boldsymbol{t}_p^{cap} + Ma\, \boldsymbol{t}_p^{mar}. \tag{4.10}$$

At each perturbation level, we apply (4.4), (4.9) to solve for the velocity field in terms of shape, f, and surfactant distribution, g. Then we determine f and g using the evolution (3.4) and (3.6).

4.2. *Expansions in spherical harmonics*

Spherical harmonics are used to represent not only the shape and surfactant distribution but also velocity and stress fields. This formalism, in particular the use of scalar and vector spherical harmonics, has already been presented in several papers (Bławzdziewicz *et al.* 2000; Vlahovska *et al.* 2005). In this section, we outline the basics and give more details about the new features related to the representation of stresses with tensor spherical harmonics.

Vector quantities such as the interfacial stress (4.10) and the normal vector (4.8) are expanded in vector spherical harmonics $\boldsymbol{y}_{jmq}(\Omega)$ (B 1):

$$\boldsymbol{t}_p = \sum_{jmq} t_{jmq,p}(\boldsymbol{f},\boldsymbol{g})\,\boldsymbol{y}_{jmq}, \qquad \boldsymbol{n}_p = \sum_{jmq} n_{jmq,p}(\boldsymbol{f},\boldsymbol{g})\,\boldsymbol{y}_{jmq}, \tag{4.11}$$

where $\boldsymbol{f}$ and $\boldsymbol{g}$ denote the sets of shape and surfactant parameters

$$\boldsymbol{f} \equiv \{f_{jm}\}, \qquad \boldsymbol{g} \equiv \{g_{jm}\} \tag{4.12}$$

and

$$\sum_{jmq} \equiv \sum_{j=2}^{\infty}\sum_{m=-j}^{j}\sum_{q=0}^{2}. \tag{4.13}$$

Velocity and stress fields are described using a basis of fundamental solutions of the Stokes equations (Cichocki, Felderhof & Schmitz 1988). The velocity basis functions are

$$\boldsymbol{u}^{\pm}_{jmq}(\boldsymbol{r}) = \sum_{q'=0}^{2} U^{\pm}_{q'q}(j;r)\,\boldsymbol{y}_{jmq'}, \tag{4.14}$$

where $U_{q'q}(j;r)$ can be found in Bławzdziewicz *et al.* (2000). There is a stress tensor field associated with each $\boldsymbol{u}^{\pm}_{jmq}$:

$$\boldsymbol{T}^{\pm}_{jmq}(\boldsymbol{r}) = -p^{\pm}_{jmq}\boldsymbol{I} + \nabla'\boldsymbol{u}^{\pm}_{jmq}, \tag{4.15}$$

where the pressure is given by (Bławzdziewicz *et al.* 2000)

$$p^{\pm}_{jmq}(\boldsymbol{r}) = P^{\pm}_{q}(j;r)\,Y_{jm}, \tag{4.16}$$

and the rate-of-strain tensor is expanded in tensor spherical harmonics $\boldsymbol{\mathcal{Y}}_{jmq}$ (B 2)

$$\nabla'\boldsymbol{u}^{\pm}_{jmq} = \sum_{q'=-2}^{2} \mathscr{U}^{\pm}_{qq'}(j;r)\,\boldsymbol{\mathcal{Y}}_{jmq'}. \tag{4.17}$$

The matrices $\mathscr{U}_{qq'}(j;r)$ are listed in Appendix B.2.

In the basis of functions (4.14), the velocity fields are represented as

$$\boldsymbol{u}^{out}(\boldsymbol{r}) = \boldsymbol{u}^{\infty} + \sum_{jmq} c^{-}_{jmq}\boldsymbol{u}^{-}_{jmq}(\boldsymbol{r}), \qquad \boldsymbol{u}^{in}(\boldsymbol{r}) = \sum_{jmq} c^{+}_{jmq}\boldsymbol{u}^{+}_{jmq}(\boldsymbol{r}). \tag{4.18}$$

The corresponding stress fields are

$$\boldsymbol{T}^{out}(\boldsymbol{r}) = \boldsymbol{E} + \sum_{jmq} c^{-}_{jmq}\boldsymbol{T}^{-}_{jmq}(\boldsymbol{r}), \qquad \boldsymbol{T}^{in}(\boldsymbol{r}) = \sum_{jmq} c^{+}_{jmq}\boldsymbol{T}^{+}_{jmq}(\boldsymbol{r}). \tag{4.19}$$

The external flow and stress are specified by

$$\boldsymbol{u}^{\infty}(\boldsymbol{r}) = \sum_{jmq} c^{\infty}_{jmq} \boldsymbol{u}^{+}_{jmq}(\boldsymbol{r}), \qquad \boldsymbol{E} = \sum_{jmq} c^{\infty}_{jmq} \boldsymbol{T}^{+}_{jmq}(\boldsymbol{r}). \tag{4.20}$$

Following the perturbation scheme (4.1), the coefficients are expanded as

$$c^{\pm}_{jmq} = \sum_{p=0}^{\infty} \varepsilon^{p} c^{\pm}_{jmq,p}(\boldsymbol{f}, \boldsymbol{g}, Ca, \chi, E). \tag{4.21}$$

Hereafter, we adopt the notation that summation over repeated indices is implied.

4.3. *Matrix representation of the boundary conditions at the deformed interface*

The spherical harmonics representation transforms the boundary conditions for the velocity (4.4) and stresses (4.9) into a matrix form. The perturbation problem reduces to solving a hierarchy of the matrix equations, which we have done using the software for symbolic computations *Mathematica*. The calculations up to (and including) order $p = 3$ were performed. However, owing to its hierarchical structure, the solution, in principle, can be extended to higher orders.

4.3.1. *Velocity*

Introducing representations (4.18) and (4.14) in the expression for the surface velocity (4.3) leads to

$$\bar{\boldsymbol{u}}^{\nu}_{p}(\Omega) = \sum_{k=0}^{p} c^{\pm}_{jmq,p-k} U^{\pm,(k)}_{qq_1}(j; r=1)\, \boldsymbol{y}_{jmq_1} \qquad \nu = in,\ \text{out}, \tag{4.22}$$

where $U^{\pm,(k)}$ denotes the kth term in the Taylor series for the $U^{\pm}_{qq_1}(j;r)$ (defined analogous to (4.3)). After some algebra, details of which are given in Appendix C.1, we obtain

$$\bar{\boldsymbol{u}}^{\nu}_{p}(\Omega) = \sum_{k=0}^{p} c^{\pm}_{jmq,p-k} \boldsymbol{D}^{\pm}_{jmqj_2m_2q_2,k}(\boldsymbol{f})\, \boldsymbol{y}_{j_2m_2q_2} \quad \nu = in,\ \text{out}. \tag{4.23}$$

The matrix $\boldsymbol{D}_{jmqj_2m_2q_2,k}$ (C 5) is diagonal at $k = 0$:

$$\boldsymbol{D}_{jmqj_2m_2q_2,0} = \delta_{j\,j_2}\delta_{m\,m_2}\delta_{q\,q_2}, \tag{4.24}$$

where δ_{nm} denotes the Kronecker delta function. Thus, according to (4.24) and (4.23), the velocity continuity condition (4.4) can be rewritten as a relation between the velocity coefficients inside and outside the drop

$$c^{+}_{jmq,p} = c^{-}_{jmq,p} + v_{jmq,p}, \tag{4.25}$$

where the term $v_{jmq,p}$ is defined to absorb all contributions from the lower order ($k < p$) perturbations

$$v_{jmq,p} = c^{\infty}_{j'm'q'} \boldsymbol{D}^{+}_{j'm'q'jmq,p}(\boldsymbol{f}) + \sum_{k=1}^{p} \left(c^{-}_{j'm'q',p-k} \boldsymbol{D}^{-}_{j'm'q'jmq,k}(\boldsymbol{f}) - c^{+}_{j'm'q',p-k} \boldsymbol{D}^{+}_{j'm'q'jmq,k}(\boldsymbol{f}) \right). \tag{4.26}$$

Equation (4.25) illustrates the recursive structure of the perturbation solution.

4.3.2. *Hydrodynamic tractions*

Similar analysis of the hydrodynamic tractions leads to an equation analogous to (4.23). The surface tractions (4.7) are cast into the form

$$\boldsymbol{\tau}_p^v(\Omega) = \sum_{k=0}^{p} c^{\pm}_{jmq,p-k} \Theta^{\pm}_{jmqj_2m_2q_2,k}(\boldsymbol{f})\, \boldsymbol{y}_{j_2m_2q_2}. \tag{4.27}$$

The traction matrices $\boldsymbol{\Theta}_k^{\pm}$ are discussed in Appendix C.2, where the explicit expressions for the perturbation order $k=1$ are listed. For $k=0$, the traction matrix reduces to

$$\Theta^{\pm}_{jmqj_2m_2q_2,0} = \delta_{jj_2}\delta_{mm_2}\Theta^{\pm}_{qq_2}(j), \tag{4.28}$$

where $\Theta^{\pm}_{qq_2}$ is given by (C 12). The stress jump condition (4.9) is rewritten in a matrix form as

$$c^{-}_{jmq',p}\Theta^{-}_{q'q}(j) - (\chi-1)c^{+}_{jmq',p}\Theta^{+}_{q'q}(j) = x_{jmq,p}, \tag{4.29}$$

where the contributions from the lower order solutions as well as the interfacial stresses and tractions due to the external flow are combined in

$$x_{jmq,p} = \sum_{k=1}^{p} \left(c^{-}_{j'm'q',p-k}\Theta^{-}_{j'm'q'jmq,k}(\boldsymbol{f}) - c^{+}_{j'm'q',p-k}\Theta^{+}_{j'm'q'jmq,k}(\boldsymbol{f})\right) - \delta_{j2}\delta_{p0}\tau^{\infty}_{jmq} + t_{jmq,p}(\boldsymbol{f},\boldsymbol{g}). \tag{4.30}$$

The last term in (4.30) is the interfacial stress expansion term $t_{jmq,p}$ from (4.11). The tractions associated with the external flow (2.1) are τ^{∞}_{jmq}.

4.4. *Problem solution: recurrence relations*

The solution at the perturbation order p is given by a recurrence relation involving the solutions at lower perturbation orders.

4.4.1. *Velocity and stress fields*

The velocity and stress boundary conditions (4.25), (4.29) represent a set of linear equations for the velocity expansion coefficients $c^{+}_{jmq,k}$ and $c^{-}_{jmq,k}$. Eliminating $c^{+}_{jmq,k}$ from these equations yields the solution for the velocity coefficients of the flow field outside the drop

$$c^{-}_{jmq,p} = z_{jmq',p}\Upsilon_{q'q}, \tag{4.31}$$

where

$$z_{jmq',p} = x_{jmq',p} - (\chi-1)v_{jmq,p}\Theta^{+}_{qq'}(j) \tag{4.32}$$

and

$$\Upsilon_{q'q} = \left[\Theta^{-}_{q'q} - (\chi-1)\Theta^{+}_{q'q}\right]^{-1}. \tag{4.33}$$

Υ is defined in Appendix C.3. Explicit expressions for the velocity coefficients at perturbation orders 0 and 1 are listed in Appendix D. The expressions for orders 2 and 3 are very lengthy; they can be found in Vlahovska (2003).

The components of effective stress $\boldsymbol{T}^d$ (2.17) are directly related to the velocity coefficients $c^{-}_{2\pm 2q}$ (Vlahovska *et al.* 2005).

4.4.2. *Shape- and surfactant-evolution equations*

The shape- and surfactant-evolution (3.8) in spherical harmonics representation (3.9) take the form

$$\dot{f}_{jm} = \sum_{p=0}^{\infty} \varepsilon^p F_{jm,p}, \qquad \dot{g}_{jm} = \sum_{p=0}^{\infty} \varepsilon^p G_{jm,p}, \tag{4.34}$$

where the dot denotes the time derivative and we have introduced

$$F_p = F_{jm,p} Y_{jm}, \qquad G_p = G_{jm,p} Y_{jm}. \tag{4.35}$$

After some algebra outlined in Appendix C.4, we find

$$F_{jm,p} = c^{\pm}_{jm2,p} + w^{\pm,F}_{jm,p} \tag{4.36}$$

and, similarly,

$$G_{jm,p} = [j\,(j+1)]^{1/2} \left(c^{\pm}_{jm0,p} + w^{\pm,\Gamma}_{jm,p}\right). \tag{4.37}$$

In the above expressions, the use of outer c^- or inner c^+ velocity coefficients yields the same results (this served as a useful check). The terms $w^{\pm}_{jm,p}$ absorb all contributions from the lower order perturbations,

$$w^{\pm,F}_{jm,p} = \sum_{k=1}^{p} c^{\pm}_{j'm'q',p-k} \boldsymbol{W}^{\pm,F}_{j'm'q'jm,k}(\boldsymbol{f}), \tag{4.38}$$

and

$$w^{\pm,\Gamma}_{jm,p} = \sum_{k=1}^{p} c^{\pm}_{j'm'q',p-k} \boldsymbol{W}^{\pm,\Gamma}_{j'm'q'jm,k}(\boldsymbol{f}, \boldsymbol{g}), \tag{4.39}$$

where the matrix $\boldsymbol{W}^{\pm,F}_{j'm'q'jm,k}$ is given by (C 29) and $\boldsymbol{W}^{\pm,\Gamma}_{j'm'q'jm,k}$ is given by (C 33). Details about its derivation can be found in Vlahovska (2003). Explicit expressions for the evolution coefficients of perturbation orders 0 and 1 are listed in Appendix D; again, orders 2 and 3 are very lengthy and can be found in Vlahovska (2003).

Thus far, we have presented the solution in a general form valid for any type of external flow. In the following sections, we give explicit results for linear flows.

5. Evolution equations

Here we list the explicit expressions for the second-order $O(Ca^{-1}\varepsilon^3, Ma\varepsilon^3)$ evolution equations or shape, surfactant and effective emulsion stresses in linear flows. The third-order expressions are very lengthy; the complete set can be downloaded from Vlahovska (2007). The hyperbolic flow $(x, -y, 0)$ does not belong to the family of linear flows described by (2.2). However, it corresponds to the straining flow, $\beta = 0$, with the flow axes rotated by $\pi/4$.

Let us split f_{jm} and g_{jm} into real and imaginary parts

$$f_{j\pm m} = f'_{jm} \pm \mathrm{i} f''_{jm} \qquad g_{j\pm m} = g'_{jm} \pm \mathrm{i} g''_{jm.} \tag{5.1}$$

For $m = 0$, the shape and surfactant parameters are real. In simple-shear flow, f'_{22}, f''_{22} and f_{20} correspond to drop deformation along the flow direction (x-axis), the straining axis $x = y$ and the vorticity direction (z-axis), respectively. Let us introduce the capillary number based on the surface tension of the surfactant-free interface

$$Ca_0 = Ca(1+E)^{-1}. \tag{5.2}$$

This would allow us to take the surfactant-free limit of our theory, $Ma = 0$. The evolution equations are

$$\begin{aligned}\dot{f}_{20} &= 2d_{11}f''_{22} + d_{12}f_{20}f''_{22} + d_{13}f''_{42} \\ &\quad + Ca_0^{-1}\left[D_1 f_{20} + D_2\left(-f_{20}^2 + 2f_{22}'^2 + 2f_{22}''^2\right)\right] \\ &\quad + Ma\left[D_{12}f_{20} + D_{13}g_{20} + D_{21}\left(-f_{20}^2 + 2f_{22}'^2 + 2f_{22}''^2\right)\right. \\ &\quad \left. + D_{22}\left(-f_{20}g_{20} + 2f'_{22}g'_{22} + 2f''_{22}g''_{22}\right)\right] \end{aligned} \tag{5.3a}$$

$$\begin{aligned}\dot{f}'_{22} &= -2\omega f''_{22} + d_{21}f'_{22}f''_{22} + d_{22}f''_{44} + Ca_0^{-1}\left[D_1 f'_{22} + 2D_2 f_{20}f'_{22}\right] \\ &\quad + Ma\left[D_{12}f'_{22} + D_{13}g'_{22} + 2D_{21}f_{20}f'_{22} + D_{22}\left(f_{20}g'_{22} + g_{20}f'_{22}\right)\right] \end{aligned} \tag{5.3b}$$

$$\begin{aligned}\dot{f}''_{22} &= 2\omega f'_{22} + \left[d_{31} + d_{11}f_{20} + d_{32}f_{20}^2 + d_{33}f_{22}'^2 + d_{34}f_{22}''^2 + d_{36}f'_{40} + d_{37}f'_{44}\right] \\ &\quad + Ca_0^{-1}\left[D_1 f''_{22} + 2D_2 f_{20}f''_{22}\right] + Ma\left[D_{12}f''_{22} + D_{13}g''_{22}\right. \\ &\quad \left. + 2D_{21}f_{20}f''_{22} + D_{22}(f_{20}g''_{22} + g_{20}f''_{22})\right] \end{aligned} \tag{5.3c}$$

$$\begin{aligned}\dot{g}_{20} &= 2b_{11}f''_{22} + 2b_{12}g''_{22} + b_{13}f_{20}f''_{22} - 2b_{14}\left(f_{20}g''_{22} - g_{20}f''_{22}\right) + b_{15}f''_{42} \\ &\quad + b_{16}g''_{42} + Ca_0^{-1}\left[-2D_{12}f_{20} + B_2\left(-f_{20}^2 + 2f_{22}'^2 + 2f_{22}''^2\right)\right. \\ &\quad \left. + B_{21}\left(-f_{20}g_{20} + 2f'_{22}g'_{22} + 2f''_{22}g''_{22}\right)\right] \\ &\quad + Ma\left[B_{12}f_{20} + B_{13}g_{20} + B_{22}\left(-f_{20}^2 + 2f_{22}'^2 + 2f_{22}''^2\right)\right. \\ &\quad \left. + B_{23}\left(-f_{20}g_{20} + 2f'_{22}g'_{22} + 2f''_{22}g''_{22}\right) + B_{24}\left(-g_{20}^2 + 2g_{22}'^2 + 2g_{22}''^2\right)\right] \end{aligned} \tag{5.3d}$$

$$\begin{aligned}\dot{g}'_{22} &= -2\omega g''_{22} + b_{21}f'_{22}f''_{22} - 2b_{14}f''_{22}g'_{22} + b_{22}f'_{22}g''_{22} + b_{17}f''_{44} + b_{18}g''_{44} \\ &\quad + Ca_0^{-1}\left[-2D_{12}f'_{22} + 2B_2 f_{20}f'_{22} + B_{21}\left(f_{20}g'_{22} + f'_{22}g_{20}\right)\right] \\ &\quad + Ma\left[B_{12}f'_{22} + B_{13}g'_{22} + 2B_{22}f_{20}f'_{22} + B_{23}\left(f_{20}g'_{22} + g_{20}f'_{22}\right)\right. \\ &\quad \left. + 2B_{24}g_{20}g'_{22}\right] \end{aligned} \tag{5.3e}$$

$$\begin{aligned}\dot{g}''_{22} &= 2\omega g'_{22} + \left[3d_{31} + b_{11}f_{20} + b_{32}f_{20}^2 + b_{33}f_{22}'^2 + b_{34}f_{22}''^2\right. \\ &\quad \left. + b_{12}g_{20} - b_{14}f_{20}g_{20} - b_{22}f'_{22}g'_{22} - 2b_{14}f''_{22}g''_{22} + b_{19}f_{40} + b_{20}g_{40}\right. \\ &\quad \left. - b_{17}f'_{44} - b_{18}g'_{44}\right] + Ca_0^{-1}\left[-2D_{12}f''_{22} + 2B_2 f_{20}f''_{22}\right. \\ &\quad \left. + B_{21}\left(f_{20}g''_{22} + f''_{22}g_{20}\right)\right] + Ma\left[B_{12}f''_{22} + B_{13}g''_{22} + 2B_{22}f_{20}f''_{22}\right. \\ &\quad \left. + B_{23}\left(f_{20}g''_{22} + g_{20}f''_{22}\right) + 2B_{24}g_{20}g''_{22}\right] \end{aligned} \tag{5.3f}$$

$$\begin{aligned}\dot{f}_{40} &= d_{41}f''_{22} + d_{42}f_{20}f''_{22} + d_{43}f''_{42} + Ca_0^{-1}\left[D_3 f_{40} + D_4\left(3f_{20}^2 + f_{22}'^2 + f_{22}''^2\right)\right] \\ &\quad + Ma\left[P_{12}f_{40} + P_{13}g_{40} + P_{21}\left(3f_{20}^2 + f_{22}'^2 + f_{22}''^2\right)\right] \\ &\quad + P_{22}(3f_{20}g_{20} + f'_{22}g'_{22} + f''_{22}g''_{22})] \end{aligned} \tag{5.3g}$$

$$\begin{aligned}\dot{f}'_{42} &= -\beta f''_{42} + d_{51}f'_{22}f''_{22} + d_{52}f''_{44} + Ca_0^{-1}[D_3 f'_{42} + D_{41}f_{20}f'_{22}] \\ &\quad + Ma[P_{12}f'_{42} + P_{13}g'_{42} + P_{31}f_{20}f'_{22} + P_{32}(f_{20}g'_{22} + g_{20}f'_{22})] \end{aligned} \tag{5.3h}$$

$$\begin{aligned}\dot{f}''_{42} &= \beta f'_{42} + d_{61}f_{20} + d_{62}f_{20}^2 + d_{63}f_{22}'^2 + d_{64}f_{22}''^2 + d_{65}f_{40} - d_{52}f'_{44} \\ &\quad + Ca_0^{-1}[D_3 f''_{42} + D_{41}f_{20}f''_{22}] + Ma[P_{12}f''_{42} + P_{13}g''_{42} \\ &\quad + P_{31}f_{20}f''_{22} + P_{32}(f_{20}g''_{22} + g_{20}f''_{22})] \end{aligned} \tag{5.3i}$$

$$\dot{f}'_{44} = -2\beta f''_{44} + d_{71} f''_{22} + d_{72} f_{20} f''_{22} + d_{73} f''_{42} + Ca_0^{-1}\left[D_3 f'_{44} + D_{42}\left(f'^2_{22} - f''^2_{22}\right)\right] + Ma\left[P_{12} f'_{44} + P_{13} g'_{44} + P_{41}\left(f'^2_{22} - f''^2_{22}\right) + P_{42}(f'_{22} g'_{22} - f''_{22} g''_{22})\right] \tag{5.3j}$$

$$\dot{f}''_{44} = 2\beta f'_{44} - d_{71} f'_{22} - d_{72} f_{20} f'_{22} - d_{73} f'_{42} + Ca_0^{-1}[D_3 f''_{44} + 2D_{42} f'_{22} f''_{22}] + Ma[P_{12} f''_{44} + P_{13} g''_{44} + 2P_{41} f'_{22} f''_{22} + P_{42}(f'_{22} g''_{22} + f''_{22} g'_{22})] \tag{5.3k}$$

$$\dot{g}_{40} = q_1 g''_{22} + q_2 g''_{42} + q_3 f''_{42} + q_{10} f_{20} f''_{22} + q_{11}(f_{20} g''_{22} - f''_{22} g_{20}) + Ca_0^{-1}\left[Q_1 f_{40} + Q_2\left(3f_{20}^2 + f'^2_{22} + f''^2_{22}\right) + Q_{22}(3f_{20} g_{20} + f'_{22} g'_{22} + f''_{22} g''_{22})\right] + Ma\left[Q_{12} f_{40} + Q_{13} g_{40} + Q_{21}\left(3f_{20}^2 + f'^2_{22} + f''^2_{22}\right) + Q_{23}(3f_{20} g_{20} + f'_{22} g'_{22} + f''_{22} g''_{22}) + Q_{24}\left(3g_{20}^2 + g'^2_{22} + g''^2_{22}\right)\right] \tag{5.3l}$$

$$\dot{g}'_{42} = -\beta g''_{42} + q_4 g''_{44} + q_5 f''_{44} + q_{12} f'_{22} f''_{22} + q_{13} f''_{22} g'_{22} + Ca_0^{-1}[Q_1 f'_{42} + Q_3 f_{20} f'_{22} + Q_{32}(f_{20} g'_{22} + g_{20} f'_{22})] + Ma[Q_{12} f'_{42} + Q_{13} g'_{42} + Q_{31} f_{20} f'_{22} + Q_{33}(f_{20} g'_{22} + g_{20} f'_{22}) + Q_{34} g_{20} g'_{22}] \tag{5.3m}$$

$$\dot{g}''_{42} = \beta g'_{42} - q_4 g'_{44} - q_5 f'_{44} + q_6 f_{40} + q_7 g_{20} + q_8 g_{40} + q_{14} f_{20}^2 + q_{15} f'^2_{22} + q_{16} f''^2_{22} + q_{17}(f''_{22} g''_{22} + \tfrac{1}{2} f_{20} g_{20}) + Ca_0^{-1}[Q_1 f''_{42} + Q_3 f_{20} f''_{22} + Q_{32}(f_{20} g''_{22} + g_{20} f''_{22})] + Ma[Q_{12} f''_{42} + Q_{13} g''_{42} + Q_{31} f_{20} f''_{22} + Q_{33}(f_{20} g''_{22} + g_{20} f''_{22}) + Q_{34} g_{20} g''_{22}] \tag{5.3n}$$

$$\dot{g}'_{44} = -2\beta g''_{44} - q_5 f''_{42} + q_9 g''_{22} - q_4 g''_{42} + q_{18} f_{20} f''_{22} + q_{19} f_{20} g''_{22} + Ca_0^{-1}\left[Q_1 f'_{44} + Q_4\left(f'^2_{22} - f''^2_{22}\right) + Q_{42}(f'_{22} g'_{22} - f''_{22} g''_{22})\right] + Ma\left[Q_{12} f'_{44} + Q_{13} g'_{44} + Q_{41}\left(f'^2_{22} - f''^2_{22}\right) + Q_{43}(f'_{22} g'_{22} - f''_{22} g''_{22}) + Q_{44}\left(g'^2_{22} - g''^2_{22}\right)\right] \tag{5.3o}$$

$$\dot{g}''_{44} = 2\beta g'_{44} + q_5 f'_{42} - q_9 g'_{22} + q_4 g'_{42} - q_{18} f_{20} f'_{22} - q_{19} f_{20} g'_{22} + Ca_0^{-1}[Q_1 f''_{44} + 2Q_4 f'_{22} f''_{22} + Q_{42}(f'_{22} g''_{22} + f''_{22} g'_{22})] + Ma[Q_{12} f''_{44} + Q_{13} g''_{44} + 2Q_{41} f'_{22} f''_{22} + Q_{43}(f'_{22} g''_{22} + f''_{22} g'_{22}) + 2Q_{44} g'_{22} g''_{22}]. \tag{5.3p}$$

In the equations above,

$$\omega = \frac{\beta}{2} - f'_{22} c_1 \tag{5.4}$$

is the angular velocity of a rigid body of the shape f in the external flow $\boldsymbol{u}^\infty$ and c_1 is a constant. The rigid-body rotation produced by the rotational flow component is given by β; $\beta = 1$ corresponds to a simple-shear flow. The remaining term represents the rigid-body rotation produced by the straining component of the flow $\boldsymbol{E}$ and vanishes for $f = 0$. The coefficients d_{ij}, b_{ij}, q_{ij} and D_{ij}, B_{ij}, P_{ij}, Q_{ij}, where $i, j = 1, 2, \ldots,$ are rational functions of the viscosity ratio χ and the elasticity E. These coefficients and the constant c_1 are listed in Appendix E. The terms that involve the coefficients d_{ij}, b_{ij} and q_{ij} represent the effect of the dissipative motion of the dispersed-phase fluid due to the straining component of the external flow; the terms that involve the coefficients D_{ij}, B_{ij}, P_{ij} and Q_{ij} represent drop relaxation towards spherical shape due to the capillary and Marangoni forces. Note that the terms associated with the external flow in equations for time derivatives of f'_{ij} (f''_{ij}) are odd (even), and

the terms associated with the interfacial forces are even (odd) with respect to the transformations (5.5)–(5.6) associated with the reversal of the direction of the flow:

$$f'_{lm} \to f'_{lm}, \quad g'_{lm} \to g'_{lm}, \tag{5.5}$$

$$f''_{lm} \to -f''_{lm}, \quad g''_{lm} \to -g''_{lm}. \tag{5.6}$$

Setting $Ma = 0$ in the shape-evolution equations yields the $O(Ca^{-1}\varepsilon^3)$ theory for a clean drop. Thus, we extend the work by Barthès-Biesel & Acrivos (1973*a*), as discussed in more detail in § (8).

The effective stress of a dilute emulsion is determined from the shape and surfactant via

$$\begin{aligned} T_{12}^d = {} & \tau_0 + \tau_{11} f_{20} + \tau_{12} f_{40} + \tau_{13} f'_{44} + \tau_{14} f_{20}^2 + \tau_{15} f'^2_{22} + \tau_{16} f''^2_{22} \\ & + Ca_0^{-1}[-4\tau_{21} f''_{22} + \tau_{22} f_{20} f''_{22}] + Ma[\tau_{21}(6f''_{22} - g''_{22}) \\ & + \tau_{31} f_{20} f''_{22} + \tau_{32}(f_{20} g''_{22} + g_{20} f''_{22})] \end{aligned} \tag{5.7}$$

$$\begin{aligned} N_1 = {} & 2\tau_{13} f'_{44} + n_{11} f'_{22} f''_{22} + 2Ca_0^{-1}[4\tau_{21} f'_{22} - \tau_{22} f_{20} f'_{22}] \\ & - 2Ma[\tau_{21}(6f'_{22} - g'_{22}) + \tau_{31} f_{20} f'_{22} + \tau_{32}(f_{20} g'_{22} + g_{20} f'_{22})] \end{aligned} \tag{5.8}$$

$$\begin{aligned} N_2 = {} & \sqrt{6}\tau_{11} f''_{22} + 3\sqrt{10}\tau_{12} f''_{42} + n_{21} f_{20} f''_{22} \\ & + \sqrt{\tfrac{3}{2}} Ca_0^{-1}\left[-4\tau_{21} f_{20} + \tau_{22}\left(f'^2_{22} + f''^2_{22} - \tfrac{1}{2} f_{20}^2\right)\right] + \sqrt{\tfrac{3}{2}} Ma\left[\tau_{21}(6f_{20} - g_{20})\right. \\ & \left. + \tau_{31}\left(f'^2_{22} + f''^2_{22} - \tfrac{1}{2} f_{20}^2\right) + 2\tau_{32}\left(f'_{22} g'_{22} + f''_{22} g''_{22} - \tfrac{1}{2} f_{20} g_{20}\right)\right]. \end{aligned} \tag{5.9}$$

The coefficients τ_{ij} and n_{ij} are rational functions of the viscosity contrast χ and E. They are listed in Appendix F.

The three-dimensional axisymmetric extensional flow $\boldsymbol{u}^\infty = (\frac{1}{2}x, \frac{1}{2}y, -z)$ represents an important type of linear flow not described by (2.2). Because of the axial symmetry $f_{jm} = 0$ and $g_{jm} = 0$ if $m \neq 0$. The evolution equations take a simpler form

$$\begin{aligned} \frac{\partial f_{20}}{\partial t} = {} & s\left(d_{31} - d_{11} f_{20} + \tfrac{1}{2} d_{34} f_{20}^2 + 6d_{36} f_{40}\right) + Ca_0^{-1}\left(D_1 f_{20} - D_2 f_{20}^2\right) \\ & + Ma\left(D_{12} f_{20} + D_{13} g_{20} - D_{21} f_{20}^2 - D_{22} f_{20} g_{20}\right) \\ \frac{\partial f_{40}}{\partial t} = {} & s\left(3d_{41} f_{20} - \sqrt{\tfrac{3}{5}} d_{64} f_{20}^2 - \tfrac{1}{3}\sqrt{\tfrac{5}{3}} d_{43} f_{40}\right) + Ca_0^{-1}\left(D_3 f_{40} + 3D_4 f_{20}^2\right) \\ & + Ma\left(P_{12} f_{20} + P_{13} g_{20} + 3P_{21} f_{20}^2 + 3P_{22} f_{20} g_{20}\right) \end{aligned} \tag{5.10}$$

$$\begin{aligned} \frac{\partial g_{20}}{\partial t} = {} & s\left(3d_{31} - b_{11} f_{20} - b_{12} g_{20} + \tfrac{1}{2} b_{34} f_{20}^2 - b_{14} f_{20} g_{20} + 6b_{19} f_{40} + 6b_{20} g_{40}\right) \\ & + Ca_0^{-1}\left(2D_{12} f_{20} - B_2 f_{20}^2 - B_{21} f_{20} g_{20}\right) \\ & + Ma\left(B_{12} f_{20} + B_{13} g_{20} - B_{22} f_{20}^2 - B_{23} f_{20} g_{20} - B_{24} g_{20}^2\right) \\ \frac{\partial g_{40}}{\partial t} = {} & s\left(3q_1 g_{20} - \sqrt{\tfrac{3}{5}} q_{16} f_{20}^2 + \sqrt{5} q_{11} f_{20} g_{20} - \tfrac{1}{3}\sqrt{\tfrac{5}{3}}(q_3 f_{40} + q_2 g_{40})\right) \\ & + Ca_0^{-1}(Q_1 f_{40} + 3Q_2 f_{20}^2 + 3Q_{22} f_{20} g_{20}) \\ & + Ma\left(Q_{12} f_{40} + Q_{13} g_{40} + 3Q_{21} f_{20}^2 + 3Q_{23} f_{20} g_{20} + 3Q_{24} g_{20}^2\right), \end{aligned} \tag{5.11}$$

where $s = -\sqrt{6}$. Note that the coefficients corresponding to relaxation driven by interfacial forces are identical to those in (5.3).

6. Weak-flow expansions for a stationary drop

We focus our attention on steady state drop deformation; however, our analysis can also be used to explore transient flows using the evolution (5.3). We present theoretical calculations for drop deformation and the effective stress of an emulsion consisting of deformable surfactant-free drops in the weak-flow limit, where the small parameter is the flow strength $\varepsilon \equiv Ca$. In the case of no viscosity contrast, $\chi = 2$, the expansions reduce to the ones derived in Vlahovska *et al.* (2005).

6.1. *Axisymmetric extensional flow*

To third order in Ca, we obtain that the steady-state shape and surfactant distribution are described by

$$\begin{aligned} f_{j0} &= f_j^{(1)}(E)\,Ca + f_j^{(2)}(E)\,Ca^2 + f_j^{(3)}(E)\,Ca^3, \\ g_{j0} &= g_j^{(1)}(E)\,Ca + g_j^{(2)}(E)\,Ca^2 + g_j^{(3)}(E)\,Ca^3. \end{aligned} \tag{6.1}$$

In irrotational flows, stationary shape and surfactant distribution are independent of the viscosity contrast, because the Marangoni stresses immobilize the surface at steady state (Milliken *et al.* 1993; Bazhlekov *et al.* 2006). At leading order, the only non-zero contributions are

$$f_2^{(1)} = \sqrt{5\,\pi}, \qquad g_2^{(1)} = \frac{(1+2E)\,\sqrt{5\,\pi}}{E}. \tag{6.2}$$

The second-order terms are

$$\begin{gathered} f_2^{(2)} = \frac{15\,\sqrt{5\,\pi}}{7}, \qquad f_4^{(2)} = \frac{45\,\sqrt{\pi}}{14} \\ g_2^{(2)} = \frac{5\,(5+17E)\,\sqrt{5\,\pi}}{14E} \qquad g_4^{(2)} = \frac{15\,(9+4E)\,\sqrt{\pi}}{14E}. \end{gathered} \tag{6.3}$$

The third-order terms are

$$\begin{gathered} f_2^{(3)} = \frac{5\,(216-49E)\,\sqrt{5\pi}}{98} \qquad f_4^{(3)} = \frac{7650\sqrt{\pi}}{539} \qquad f_6^{(3)} = \frac{5625\sqrt{\pi/13}}{308} \\ g_2^{(3)} = \frac{5\left(199+1518E-196\,E^2\right)\,\sqrt{5\pi}}{196\,E} \qquad g_4^{(3)} = \frac{75\,(278+213E)\,\sqrt{\pi}}{539\,E} \\ g_6^{(3)} = \frac{1125\,(27-8E)\,\sqrt{\pi/13}}{308\,E}. \end{gathered} \tag{6.4}$$

6.2. *Simple-shear flow*

To third order in Ca, the steady-state shape and surfactant distribution for a drop in shear flow are described by the expansions

$$\begin{aligned} f_{jm} &= f_{jm}^{(1)}(E,\chi)\,Ca + f_{jm}^{(2)}(E,\chi)\,Ca^2 + f_{jm}^{(3)}(E,\chi)\,Ca^3, \\ g_{jm} &= g_{jm}^{(1)}(E,\chi)\,Ca + g_{jm}^{(2)}(E,\chi)\,Ca^2 + g_{jm}^{(3)}(E,\chi)\,Ca^3. \end{aligned} \tag{6.5}$$

The rotational component of the flow continuously redistributes the surfactant and, therefore, the stationary state of the drop will, in principle, depend on the viscosity contrast. The convergence radius for these weak-flow expansions is best for moderate viscosity contrasts. Here we list only deformation parameters with $j \leqslant 4$. At leading order, the solution is independent of viscosity contrast

$$f_{22}^{\prime\prime(1)} = -\sqrt{\frac{5\pi}{6}}, \quad g_{22}^{\prime\prime(1)} = -\frac{1+2E}{E}\sqrt{\frac{5\pi}{6}}. \tag{6.6}$$

The effect of rotation, and thus viscosity contrast, enter at second order and the non-zero contributions are

$$f_{20}^{(2)} = -\frac{5}{7}\sqrt{5\pi},\ f_{22}^{\prime(2)} = \frac{1}{24}\frac{3+\chi+E\,(9+23\chi)}{E}\sqrt{\frac{5\pi}{6}},$$
$$f_{40}^{(2)} = \frac{5}{28}\sqrt{\pi},\quad f_{44}^{\prime(2)} = -\frac{5}{4}\sqrt{\frac{5\pi}{14}}, \tag{6.7}$$

and

$$g_{20}^{(2)} = -\frac{5}{42}\frac{5+17E}{E}\sqrt{5\pi},\ g_{22}^{\prime(2)} = \frac{1}{12}\frac{10\chi+3E\,(3+\chi)+E^2\,(9+23\chi)}{E^2}\sqrt{\frac{5\pi}{6}},$$
$$g_{40}^{(2)} = \frac{5}{84}\frac{9+4E}{E}\sqrt{\pi},\qquad g_{44}^{\prime(2)} = -\frac{5}{12}\frac{9+4E}{E}\sqrt{\frac{5\pi}{14}}. \tag{6.8}$$

Note that the expressions for $f_{22}^{\prime(2)}$ and $g_{22}^{\prime(2)}$ in the $\chi = 2$ case listed in Vlahovska *et al.* (2005) contain typographical errors. At third order, the non-zero contributions are

$$f_{22}^{\prime\prime(3)} = \frac{1}{28\,224}\frac{S_1(E,\chi)}{E^2}\sqrt{\frac{5\pi}{6}},$$
$$f_{42}^{\prime\prime(3)} = \frac{425}{539}\sqrt{\frac{5\pi}{2}}, \tag{6.9}$$
$$f_{44}^{\prime\prime(3)} = -\frac{-10\,(1+\chi)+E\,(239+109\chi)+E^2\,(839+2049\chi)}{864E^2}\sqrt{\frac{5\pi}{14}},$$

and

$$g_{22}^{\prime\prime(3)} = \frac{1}{14\,112}\frac{S_2(E,\chi)}{E^3}\sqrt{\frac{5\pi}{6}},$$
$$g_{42}^{\prime\prime(3)} = \frac{25}{3234}\frac{278+213E}{E}\sqrt{\frac{5\pi}{2}},$$
$$g_{44}^{\prime\prime(3)} = -\frac{-540\chi+E\,(385+2731\chi)+E^2\,(3133+3779\chi)+2E^3\,(569+1359\chi)}{864E^3}\sqrt{\frac{5\pi}{14}}, \tag{6.10}$$

where

$$\begin{aligned} S_1(E,\chi) &= 980\chi(3+\chi)+147E(21+34\chi+9\chi^2)\\ &\quad +E^2(-99\,711+20\,286\chi+25\,921\chi^2)+23\,520E^3\\ S_2(E,\chi) &= 9800\chi^2+98E(9+96\chi+31\chi^2)+E^2(-18\,147+12\,642\chi\\ &\quad +3577\chi^2)+E^3(-178\,191+20\,286\chi+25\,921\chi^2)+23\,520E^4. \end{aligned} \tag{6.11}$$

Substituting the shape and surfactant expansions (6.5) in (5.7) yields for the effective shear viscosity a dilute emulsion

$$T_{12}^{d} = \frac{5}{2} - \frac{5}{1176E^2}[245\chi+98E(3+\chi)+E^2(-1059+1127\chi)]Ca^2. \tag{6.12}$$

At very low shear rates an emulsion of surfactant-covered drops behaves as a suspension of rigid spheres with viscosity given by Einstein's result, $1+5/2\phi$ and zero

normal stresses. Shape deformation and surfactant redistribution at increasing shear rate give rise to shear thinning, which depends on the viscosity contrast. However, at leading order the normal stresses are independent of viscosity contrast

$$\begin{aligned} N_1 &= \frac{5}{2}\frac{4E+1}{E}\,Ca, \\ N_2 &= -\frac{1}{2}N_1 + \frac{75}{28}\,Ca. \end{aligned} \tag{6.13}$$

Given that stresses are normalized by the viscous stress $\eta\dot{\gamma}$, the rheology is obtained at one order less than the drop shape and surfactant distribution. For example, the $O(Ca^3)$ term in the expansion of the normal stresses depends on the $O(Ca^4)$ perturbation in shape and surfactant.

6.3. *Surfactant-free drop*

For the sake of completeness, we list the expansions for the stationary shapes of surfactant-free drop. A comparison of the drop shapes in the absence and the presence of surfactant can provide a quantitative estimate the importance of surfactant effects.

6.3.1. *Axisymmetric extensional flow*

The third-order expansion for a surfactant-free drop in extensional flow reads

$$f_{j0} = f_j^{(1)}(\chi)\,Ca + f_j^{(2)}(\chi)\,Ca^2 + f_j^{(3)}(\chi)\,Ca^3. \tag{6.14}$$

The expansion coefficients depend on viscosity contrast

$$\begin{aligned} f_2^{(1)} &= D_T\sqrt{5\pi} \\ f_2^{(2)} &= D_T\frac{-36-309\,\chi+601\,\chi^2}{280\,\chi^2}\sqrt{5\pi} \\ f_4^{(2)} &= D_T\frac{-95+751\,\chi}{252\chi}\sqrt{\pi} \\ f_2^{(3)} &= D_T\frac{7776+115\,528\,\chi-195\,631\,\chi^2-2\,862\,098\,\chi^3+3\,220\,761\,\chi^4}{235\,200\,\chi^4}\sqrt{5\pi} \\ f_4^{(3)} &= D_T\frac{639\,780+595\,807\,\chi-51\,008\,602\,\chi^2+85\,699\,543\,\chi^3}{6\,985\,440\,\chi^3}\sqrt{5\pi} \\ f_6^{(3)} &= D_T\frac{31\,449-628\,546\,\chi+2\,934\,377\,\chi^2}{192\,192\chi^2}\sqrt{\frac{\pi}{13}}, \end{aligned} \tag{6.15}$$

where D_T is Taylor's deformation parameter (Taylor 1934):

$$D_T = \frac{(-3+19\,\chi)}{20\,\chi}. \tag{6.16}$$

6.3.2. *Simple-shear flow*

The expansion for the shape parameters of a surfactant-free drop in shear flow is

$$f_{jm} = f_{jm}^{(1)}(\chi)\,Ca + f_{jm}^{(2)}(\chi)\,Ca^2 + f_{jm}^{(3)}(\chi)\,Ca^3. \tag{6.17}$$

At leading order, the only non-zero contribution is

$$f_{22}^{\prime\prime(1)} = -D_T\sqrt{\frac{5\pi}{6}}. \tag{6.18}$$

The second-order expansion terms are

$$f_{20}^{(2)} = D_T \frac{(36 + 309\chi - 601\chi^2)}{168\chi^2}\sqrt{\frac{\pi}{5}}, \qquad f_{22}^{\prime(2)} = D_T^2 \frac{2\chi + 1}{2}\sqrt{\frac{5\pi}{6}},$$
$$f_{40}^{(2)} = D_T \frac{-95 + 751\chi}{4536\chi}\sqrt{\pi}, \qquad f_{44}^{\prime(2)} = D_T \frac{95 - 751\chi}{648\chi}\sqrt{\frac{5\pi}{14}}. \tag{6.19}$$

At third order, we have

$$f_{22}^{\prime\prime(3)} = D_T \frac{(-1944 - 28\,882\chi + 49\,900\chi^2 + 706\,925\chi^3 - 811\,695\chi^4 + 108\,927\chi^5 + 159\,201\chi^6)}{35\,280\chi^4}\sqrt{\frac{\pi}{30}},$$
$$f_{42}^{\prime\prime(3)} = D_T \frac{639\,780 + 595\,807\chi - 51\,008\,602\chi^2 + 85\,699\,543\chi^3}{25\,147\,584\chi^3}\sqrt{\frac{\pi}{10}}, \tag{6.20}$$
$$f_{44}^{\prime\prime(3)} = -D_T \frac{5077 - 62\,376\chi + 119\,505\chi^2 + 507\,394\chi^3}{46\,656\chi^2}\sqrt{\frac{\pi}{70}}.$$

The expansions for the effective stresses of a dilute emulsion (5.7)–(5.9) are

$$T_{12}^d = \frac{5}{2} - \frac{3}{2\chi} - Ca^2 D_T(\chi) \times \frac{-3888 - 27\,308\chi + 231\,041\chi^2 - 33\,637\chi^3 - 189\,761\chi^4 + 159\,201\chi^5}{35\,280\chi^4}$$
$$N_1 = Ca\left(10 D_T^2\right), \tag{6.21}$$
$$N_2 = -\tfrac{1}{2}N_1 - Ca\, D_T \frac{3(12 + 9\chi - 25\chi^2)}{28\chi^2}.$$

The expressions for the normal stresses agree with Schowalter, Chaffey & Brenner (1968). The shear thinning coefficient differs from Barthès-Biesel & Acrivos (1973*b*), but this can be attributed to the fact that the $O(\varepsilon^3)$ theory of these authors was incomplete (see § 8).

7. Discussion

The results presented in the previous section show that the presence of surfactant suppresses the sensitivity of the stationary state to viscosity contrast. However, the transient dynamics strongly depends on viscosity contrast as illustrated in figure 2: higher drop viscosities slow the approach to the steady state.

In axisymmetric extensional flow, the stationary deformation of a surfactant-covered drop is independent of viscosity ratio in contrast to a surfactant-free drop, see (6.15). Marangoni stresses immobilize the interface at steady state. Hence, the surface velocity vanishes and there is no fluid flow inside the drop. Surfactant enhances drop deformation; in the high-viscosity limit, $\chi \to \infty$, the deformation of a clean drop is smaller than a surfactant-covered one by a factor of 19/20 (at leading order).

Drop deformation in a simple-shear flow is illustrated in figure 3, where the predictions from the small-deformation theory are compared to numerical simulations using the boundary integral method (Vlahovska *et al.* 2005). In weak flows, the stationary state is independent of viscosity contrast at leading order; the drop feels only the extensional component of the flow and the Marangoni stresses rigidify the interface. The effect of viscosity contrast enters at second order because of the rotational component of the flow acting on the deformed drop. The rotation continuously redistributes the surfactant, thereby remobilizing the interface. In strong

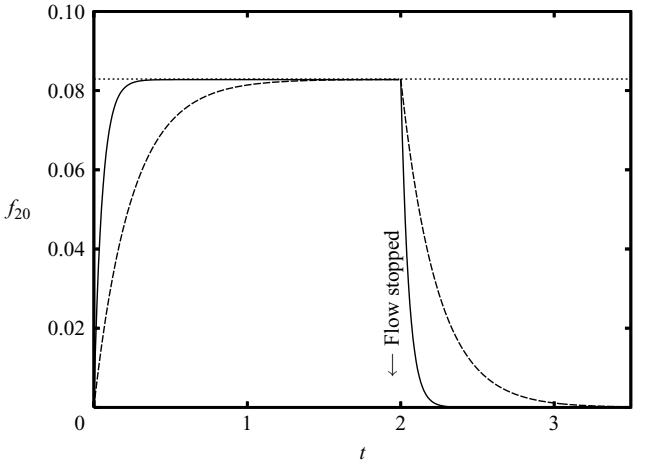

FIGURE 2. Drop shape evolution upon startup and cessation of axisymmetric extensional flow with $Ca = 0.02$ and $E = 1$ for two different viscosity ratios, $\chi = 2$ (solid line) and $\chi = 11$ (dashed line). The dotted line shows the stationary deformation.

flows, the effect of viscosity contrast is more pronounced as the numerical results in figure 3 indicate.

Experiments typically characterize drop response to shear flow by a deformation parameter, D, and the inclination angle with respect to the flow direction, ϕ_0. D is defined as $(L-B)/(L+B)$, where $L = r(\phi_0)$ and $B = r(\phi_0 + \pi/2)$ are the drop lengths along the main and minor axes of the ellipsoidal drop contour in the flow plane. Using (3.1) and the expansions for the stationary shape parameters (6.5), we obtain

$$\phi_0 = \frac{\pi}{4} - Ca\left[\frac{(23\chi+9)E+\chi+3}{48E}\right] + Ca^2\left[\frac{(21\chi-29)E^2+(31-19\chi)E+10(\chi+1)}{1152E^2}\right]. \quad (7.1)$$

The long and short axes, r_+ and r_- respectively, are

$$r_\pm = 1 \pm Ca\frac{5}{4} + Ca^2\frac{1175}{672} \mp Ca^3\frac{5}{2\,483\,712E^2}[1617(13\chi^2+38\chi-3) + 517\,440E^3 + (285\,131\chi^2+223\,146\chi-2\,971\,701)E^2 + 4312(\chi+3)^2E]. \quad (7.2)$$

Accordingly, $L = 2r_+$, $B = 2r_-$ and the deformation parameter is

$$D = Ca\frac{5}{4} + \frac{5Ca^3}{2\,483\,712E^2} \times [517\,440E^3 + (285\,131\chi^2+223\,146\chi-1\,886\,001)E^2 + 4312(\chi+3)^2E + 1617(13\chi^2+38\chi-3)] + O(Ca^4). \quad (7.3)$$

The leading-order deformation is independent of the elasticity and viscosity ratio. The theory agrees well with experimental data, as shown in figures 4 and 5.

The rheology of a dilute emulsion of surfactant-covered deformable drops is shown in figures 6 and 7. The results predict a shear-thinning viscosity, a positive first normal stress difference and a negative second normal stress difference, as generally observed in emulsions. Drop deformation and surfactant redistribution both contribute to these non-Newtonian features. In weak flows, the surfactant immobilizes the interface so

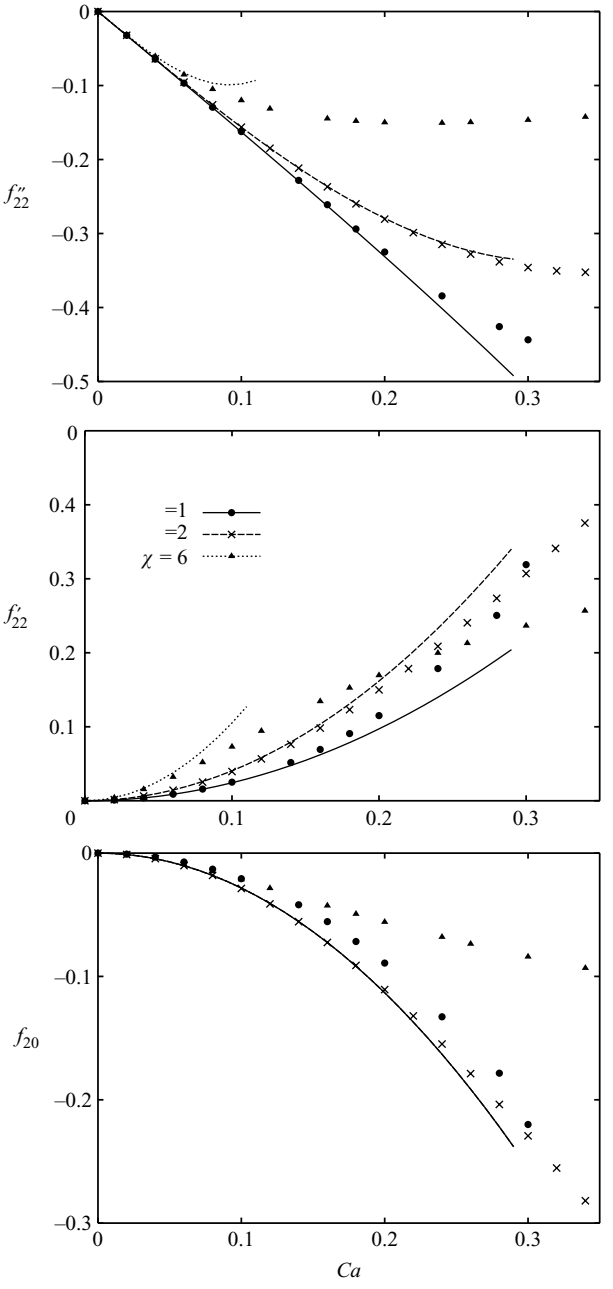

FIGURE 3. Drop deformation in a simple-shear flow: The shape parameters f''_{22}, f'_{22} and f'_{20} as a function of the flow strength Ca for a surfactant-covered drop with elasticity $E = 1$ and viscosity contrast: $\chi = 1$ (circles, solid line), $\chi = 2$ (crosses, dashed line), $\chi = 6$ (triangles, dotted line). The points are data from boundary integral simulations. The lines represent the third-order small-deformation theory (6.5).

that the emulsion behaves as a suspension of rigid spheres at leading order. The viscosity contrast affects the rheology at second order because of the tendency for the rotational component of the flow to align the deformed drop with the velocity. Drop alignment increases with viscosity contrast leading to enhanced shear thinning

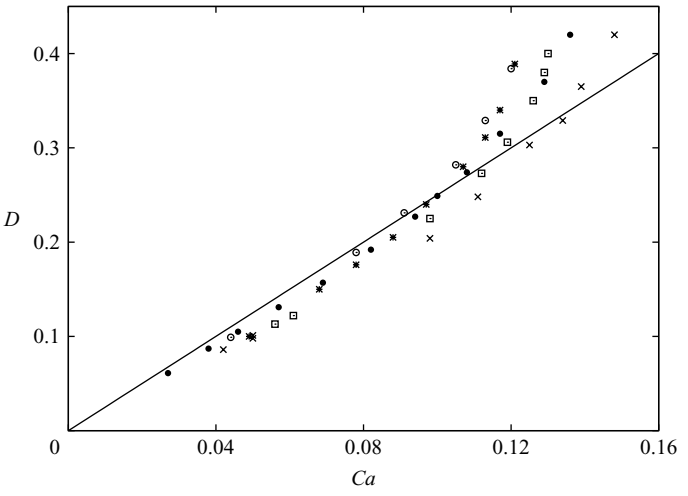

FIGURE 4. Steady drop deformation in an extensional flow $\boldsymbol{u}^{\infty} = (x, -y, 0)$ (Hu & Lips 2003). Points are experimental data for various surfactant coverage and viscosity contrasts $\chi = 1.093$ and $\chi = 3.3$. The theoretical line is $D = 5/2Ca$.

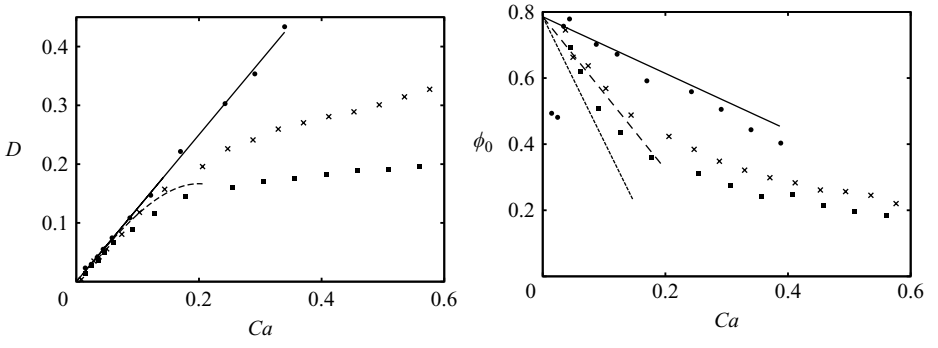

FIGURE 5. Steady deformation and inclination angle of a surfactant-covered drop in a simple shear flow (Feigl *et al.* 2007). Points are experimental data for viscosity contrasts $\chi = 1.335$ (circles), $\chi = 4.335$ (crosses), and $\chi = 7.338$ (squares). The theoretical lines are given by (7.3) and (7.1).

as predicted by (7.1). In strong flows, the effect of viscosity contrast is more visible as the numerical results in figure 3 indicate. Our numerical results agree qualitatively with the simulations of Yon & Pozrikidis (1998); however, quantitative comparison is not possible because the simulations include surfactant diffusion. Our theory quantitatively describes the rheology, although the radius of convergence of expansions (6.12) and (6.13) is apparently small, as indicated by the results in figures 6 and 7.

8. Relation to previous small-deformation analyses

The classic works on deformation of surfactant-free drops (Chaffey & Brenner 1967; Cox 1969; Frankel & Acrivos 1970; Barthès-Biesel & Acrivos 1973*a*) employ a tensorial representation of the spherical harmonics. A spherical harmonic of order j is a symmetric traceless Cartesian tensor of jth order, having $(2j + 1)$-independent

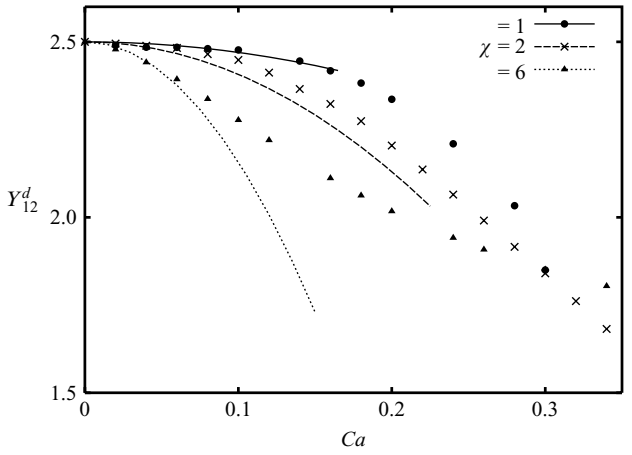

FIGURE 6. Effective shear viscosity as a function of the flow strength Ca for an emulsion of surfactant-covered drops with elasticity $E = 1$ and different viscosity contrasts: $\chi = 1$ (circles, solid line), $\chi = 2$ (crosses, dashed line), $\chi = 6$ (triangles, dotted line). The points are data from boundary integral simulation. The lines represent the third-order small-deformation theory (6.12).

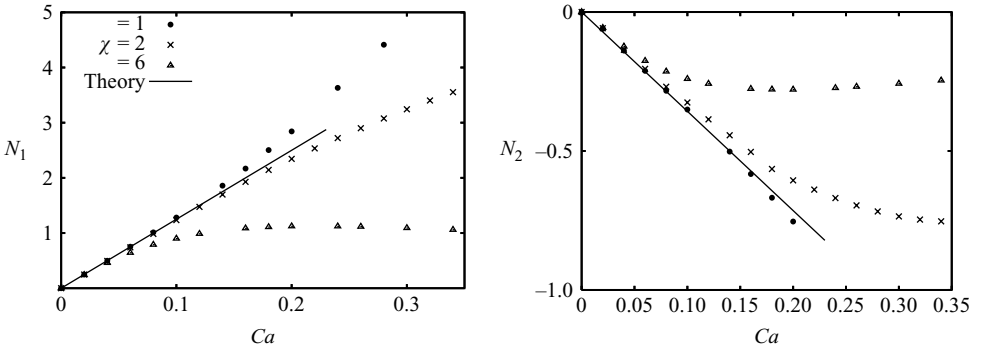

FIGURE 7. Normal stress differences N_1 and N_2 as a function of the flow strength Ca for an emulsion of surfactant-covered drops with elasticity $E = 1$ and different viscosity contrasts: $\chi = 1$ (circles), $\chi = 2$ (crosses), $\chi = 6$ (triangles). The points are data from boundary integral simulation. The lines represent the small-deformation theory (6.13).

components

$$\Psi_j(\Omega) = \nabla^j \left(\frac{1}{r}\right), \tag{8.1}$$

where ∇^j denotes applying the gradient operator j times.

The correspondence between the $2j + 1$ components of the Cartesian tensor (8.1) and the $2j + 1$ scalar harmonics Y_{jm} $(m = -j, \ldots, j)$ defined by (A 1) is discussed in Appendix A; for more details the reader is also referred to Vlahovska (2003). We have found that the scalar harmonics offered a less complex way to perform the calculations for the higher order perturbations, because there is a very well-developed

theory for manipulating the products of spherical harmonics (Jones 1985; Varshalovich, Moskalev & Kheronskii 1988).

In this section, we translate the shape-evolution equations from a tensorial form (Rallison 1980) to our scalar spherical harmonics representation. The motivation is to ease the communication between researchers that are more accustomed to either notation. The perturbation f of the drop shape (3.1) in the tensorial form reads

$$f = \varepsilon 3\boldsymbol{F}_2 : \hat{\boldsymbol{r}}\hat{\boldsymbol{r}} + \varepsilon^2 \left[-\frac{6}{5}\boldsymbol{F}_2 : \boldsymbol{F}_2 + 105\boldsymbol{F}_4 \vdots \hat{\boldsymbol{r}}\hat{\boldsymbol{r}}\hat{\boldsymbol{r}}\hat{\boldsymbol{r}} \right] + O(\varepsilon^3), \tag{8.2}$$

where $\boldsymbol{F}_j$ is a fully symmetric traceless tensor of the order j. Extending the analysis of Barthès-Biesel & Acrivos (1973*a*), the following evolution equations for the second- and fourth-order tensors are obtained:

$$\varepsilon \frac{\partial \boldsymbol{F}_j}{\partial t} = \boldsymbol{L}_j, \tag{8.3}$$

where

$$\begin{aligned} \boldsymbol{L}_2 = & -\hat{\boldsymbol{\Omega}}\boldsymbol{F}_2 + a_0\boldsymbol{E} + \varepsilon\,[\kappa a_1 \boldsymbol{F}_2 + a_2 \mathrm{Sd}(\boldsymbol{E}\cdot\boldsymbol{F}_2)] \\ & + \varepsilon^2 \left[\kappa a_3 \mathrm{Sd}\left(\boldsymbol{F}_2^2\right) + a_4 \boldsymbol{E}\boldsymbol{F}_2 : \boldsymbol{F}_2 + a_5 \boldsymbol{F}_2\boldsymbol{E} : \boldsymbol{F}_2 + a_7 \mathrm{Sd}\left(\boldsymbol{E}\cdot\boldsymbol{F}_2^2\right) + a_8 \boldsymbol{F}_4 : \boldsymbol{E}\right] \\ & + \varepsilon^3\kappa\,(a_6 \boldsymbol{F}_2\boldsymbol{F}_2 : \boldsymbol{F}_2 + a_9 \boldsymbol{F}_2 : \boldsymbol{F}_4) + O(\varepsilon^3), \end{aligned} \tag{8.4}$$

and

$$\begin{aligned} \boldsymbol{L}_4 = & -\hat{\boldsymbol{\Omega}}\boldsymbol{F}_4 + b_1 \mathrm{Sd}_4(\boldsymbol{E}\boldsymbol{F}_2) + \varepsilon\,[\kappa b_0 \boldsymbol{F}_4 + \kappa b_2 \mathrm{Sd}_4(\boldsymbol{F}_2\boldsymbol{F}_2) + b_3 \mathrm{Sd}_4(\boldsymbol{E}\cdot\boldsymbol{F}_4) \\ & + b_4 \mathrm{Sd}_4(\boldsymbol{E}\cdot\boldsymbol{F}_2\boldsymbol{F}_2) + b_5 \mathrm{Sd}_4(\boldsymbol{F}_2\cdot\boldsymbol{F}_2\boldsymbol{E})] \\ & + \varepsilon^2\kappa\,[b_6 \mathrm{Sd}_4(\boldsymbol{F}_2\cdot\boldsymbol{F}_2\boldsymbol{F}_2) + b_7 \mathrm{Sd}_4(\boldsymbol{F}_2\cdot\boldsymbol{F}_4)] + O(\varepsilon^2). \end{aligned} \tag{8.5}$$

In the above equations, $\kappa = Ca^{-1}$, the deviatoric operators Sd and $\frac{1}{3}\mathrm{Sd}_4$ represent the fully symmetric traceless parts of the corresponding second- and fourth-order tensors and the operator $\hat{\boldsymbol{\Omega}}$ represents rigid-body rotation of the drop due to the rotational component of the flow. Note that Rallison (1980) omitted the term proportional to b_5 in his analysis; however, there are two independent ways to couple $\boldsymbol{E}$ and two tensors $\boldsymbol{F}_2$ to obtain a fourth-order tensor. The complete set of shape equations at $O(\varepsilon^3)$ should also include the sixth-order tensor $\boldsymbol{F}_6$. However, the steady-state rheology is not affected by $\boldsymbol{F}_6$, and we omit it for the sake of keeping the presentation concise.

The expressions for the coefficient $a_0, \ldots, a_9$ and $b_0, \ldots, b_2$ were derived by Barthès-Biesel & Acrivos (1973*a*). Note that there is a misprint in the expression for b_2, 431 should read 413. The expression for a_9 should be corrected to

$$a_9 = \frac{80\left(81\,052\chi^5 + 68\,132\chi^4 + 10\,203\chi^3 - 20\,850\chi^2 + 135\chi + 80\right)}{21(2\chi+1)^2(10\chi+1)(17\chi-1)(19\chi-3)^2}. \tag{8.6}$$

We obtain for the coefficients b_3, b_4, b_5, b_6 and b_7, needed for a consistent $O(Ca^2)$ theory, the following expressions:

$$b_3 = \frac{20(-29+4\chi)}{11(1+2\chi)(1+10\chi)},$$
$$b_4 = \frac{288(-2+\chi)(-2+29\chi)}{539(1+2\chi)^2(1+10\chi)},$$
$$b_5 = \frac{72(-2+\chi)}{77(1+2\chi)(1+10\chi)}, \tag{8.7}$$
$$b_6 = \frac{20P(\chi)}{231(1+2\chi)^2(1+10\chi)^2(-1+17\chi)^2(-3+19\chi)^2},$$
$$b_7 = \frac{20\left(2\,715\,400\chi^5 + 1\,976\,946\chi^4 - 468\,621\chi^3 - 140\,120\chi^2 + 13\,143\chi + 276\right)}{77(2\chi+1)(10\chi+1)^2(17\chi-1)^2(19\chi-3)},$$

where

$$P(\chi) = 15\,156 + 577\,947\chi - 11\,326\,093\chi^2 + 16\,345\,769\chi^3 + 247\,274\,201\chi^4 - 997\,178\,008\chi^5 + 1\,392\,085\,940\chi^6 - 485\,298\,400\chi^7. \tag{8.8}$$

The perturbation solution at $p \leqslant 2$ for a surfactant-free drop agrees with the second-order theory derived by Barthès-Biesel & Acrivos (1973*a*). Greco (2002) reported some discrepancies with Barthès-Biesel & Acrivos (1973*a*), which we do not find. Moreover, we have carefully checked the coefficients with boundary-integral numerical simulations of drop deformation in axisymmetric extensional flow as well as with the theory for equiviscous drop (Vlahovska *et al.* 2005).

9. Conclusions

A perturbation solution of order $O(\varepsilon^3)$, where ε measures the magnitude of the shape distortion, was developed to describe the dynamics of a deformable surfactant-covered drop with arbitrary surfactant elasticity and viscosity contrast in creeping flows. The solution is applicable to any linear flow under transient or steady-state conditions. Spherical harmonics are employed to cast the problem into a matrix form that facilitates the application of the boundary conditions on the interface of the deformed drop. Our analysis also extends the solutions of Barthès-Biesel & Acrivos (1973*a*) for a surfactant-free drop by adding the $\varepsilon^3 Ca^{-1}$ terms.

Weak-flow expansions $O(Ca^3)$ for the stationary drop shapes in linear flows and effective stress of a dilute emulsion were derived. Predictions of drop shape, surfactant distribution and emulsion rheology based on our small-deformation theory are in quantitative agreement with our numerical simulations using the boundary integral method, although the weak-flow expansion was found to have a relatively small radius of convergence. A more efficient expansion based on the inverse viscosity contrast will be reported in a forthcoming paper.

Our analysis provides a suitably accurate theory for experimental determination of interfacial tension between immiscible polymers using drop deformation methods (Hu 2008). Surfactants affect the collective drop dynamics in non-dilute systems, e.g. hydrodynamic interactions and drop coalescence (Hu, Pine & Leal 2000; Ha, Yoon & Leal 2003; Hudson, Jamieson & Burkhart 2003; Rother & Davis 2004; Van Hemelrijck *et al.* 2004; Rother, Zinchenko & Davis 2006) and modify emulsion rheology (Pozrikidis 2001). The analytical results can serve to validate numerical simulations of flow of many surfactant-covered drops. The theory also provides a rigorous basis for studying the dynamics of other deformable particles with interfaces

that develop Marangoni stresses such as vesicles and biological cells (Seifert 1999; Misbah 2006; Vlahovska & Gracia 2007; Lebedev, Turitsyn & Vergeles 2007).

Appendix A. Transformation between scalar and tensor spherical-harmonics representation

The normalized spherical scalar harmonics are defined as

$$Y_{jm}(\Omega) = \left[\frac{2j+1}{4\pi}\frac{(j-m)!}{(j+m)!}\right]^{1/2}(-1)^m P_j^m(\cos\theta)\mathrm{e}^{\mathrm{i}m\varphi}, \tag{A 1}$$

where (r,θ,φ) are the spherical coordinates and $P_j^m(\cos\theta)$ are the Legendre polynomials; the index m takes $2j+1$ values from $-j$ to j.

To translate (8.3)–(8.5) into the spherical-harmonics representation (4.34), we introduce spherical tensors $\boldsymbol{T}_{lm}$, defined by the relations

$$Y_{2m} = \boldsymbol{T}_{2m} : \hat{\boldsymbol{r}}\hat{\boldsymbol{r}}, \tag{A 2}$$

$$Y_{4m} = \boldsymbol{T}_{4m} \vdots \hat{\boldsymbol{r}}\hat{\boldsymbol{r}}\hat{\boldsymbol{r}}\hat{\boldsymbol{r}}. \tag{A 3}$$

The real and imaginary components of $\boldsymbol{T}_{lm}$ are given by

$$\boldsymbol{T}_{lm} = \frac{1}{\sqrt{2}}(\boldsymbol{T}'_{lm} + \mathrm{i}\boldsymbol{T}''_{lm}), \tag{A 4}$$

where $\boldsymbol{T}'_{lm}$ and $\boldsymbol{T}''_{lm}$ are real. Tensors $\boldsymbol{T}'_{lm}$ and $\boldsymbol{T}''_{lm}$, where $m=0,\ldots,l$, form an orthonormal basis in the space of fully symmetric traceless tensors of the order l, with the normalization of the scalar products for $l=2,4$ given by

$$\frac{8\pi}{15}\,\boldsymbol{T}^{(i)}_{2m} : \boldsymbol{T}^{(i')}_{2m'} = \delta_{mm'}\delta_{ii'}, \tag{A 5}$$

$$\frac{32\pi}{315}\,\boldsymbol{T}^{(i)}_{4m} \vdots \boldsymbol{T}^{(i')}_{4m'} = \delta_{mm'}\delta_{ii'}, \tag{A 6}$$

where $\boldsymbol{T}^{(1)}_{lm} \equiv \boldsymbol{T}'_{lm}$ and $\boldsymbol{T}^{(2)}_{lm} \equiv \boldsymbol{T}''_{lm}$.

Consistently with (3.9) and (A 2)–(A 4), stationary drop shapes are described by tensors $\boldsymbol{T}$ with even values of the index m. Explicit expressions for non-vanishing matrix elements of the tensors $\boldsymbol{T}'_{lm}$ and $\boldsymbol{T}''_{lm}$, with $l=2,4$ and $m=2k$, are

$$\boldsymbol{T}'^{11}_{20} = \boldsymbol{T}'^{22}_{20} = -\tfrac{1}{2}\boldsymbol{T}'^{33}_{20} = -\frac{1}{4}\left(\frac{5}{\pi}\right)^{1/2}, \tag{A 7a}$$

$$\boldsymbol{T}'^{11}_{22} = -\boldsymbol{T}'^{22}_{22} = \frac{1}{4}\left(\frac{15}{\pi}\right)^{1/2}, \tag{A 7b}$$

$$\boldsymbol{T}''^{12}_{22} = \frac{1}{4}\left(\frac{15}{\pi}\right)^{1/2}. \tag{A 7c}$$

Note that the superscript indices denote the Cartesian tensor component. The fourth-order tensors are

$$\frac{1}{3}\boldsymbol{T}'^{1111}_{40} = \frac{1}{3}\boldsymbol{T}'^{2222}_{40} = \frac{1}{8}\boldsymbol{T}'^{3333}_{40} = \boldsymbol{T}'^{1122}_{40} = -\frac{1}{4}\boldsymbol{T}'^{1133}_{40} = -\frac{1}{4}\boldsymbol{T}'^{2233}_{40} = \frac{3}{16}\left(\frac{1}{\pi}\right)^{1/2}, \tag{A 8a}$$

$$\boldsymbol{T}'^{1111}_{42} = -\boldsymbol{T}'^{2222}_{42} = -\boldsymbol{T}'^{1133}_{42} = \boldsymbol{T}'^{2233}_{42} = -\frac{3}{8}\left(\frac{5}{\pi}\right)^{1/2}, \tag{A 8b}$$

$$\boldsymbol{T}'^{1112}_{42} = \boldsymbol{T}'^{2221}_{42} = -\tfrac{1}{2}\boldsymbol{T}'^{1233}_{42} = -\frac{3}{16}\left(\frac{5}{\pi}\right)^{1/2}, \tag{A 8c}$$

$$\boldsymbol{T}'^{1111}_{44} = \boldsymbol{T}'^{2222}_{44} = -\boldsymbol{T}'^{1122}_{44} = \frac{3}{16}\left(\frac{35}{\pi}\right)^{1/2}, \tag{A 8d}$$

$$\boldsymbol{T}'^{1222}_{44} = -\boldsymbol{T}'^{2111}_{44} = -\frac{3}{16}\left(\frac{35}{\pi}\right)^{1/2}; \tag{A 8e}$$

the remaining non-zero elements are obtained by permutations of the components.

According to (A 2)–(A 4) and having in mind that there are no contributions from odd l or m, the relation between (3.9) and (8.2) of the drop shape is

$$n_j \boldsymbol{F}_j = \sum_{k=1}^{j/2}\sum_{n=0}^{k}(f'_{2k\,2n}\boldsymbol{T}'_{2k\,2n} + f''_{2k\,2n}\boldsymbol{T}''_{2k\,2n}), \tag{A 9}$$

where $n_2 = 3$ and $n_4 = 105$ are the normalization factors, see (8.2). Evolution equations for the coefficients $f^{(i)}_{jm} = f'_{jm}$, f''_{jm}, $j = 2, 4$ are obtained using relations

$$\frac{\partial f^{(i)}_{2m}}{\partial t} = \frac{8\pi}{15}\,\boldsymbol{T}^{(i)}_{2m} : \boldsymbol{L}_2, \quad m = 0, 2, \tag{A 10}$$

and

$$\frac{\partial f^{(i)}_{4m}}{\partial t} = \frac{32\pi}{315}\,\boldsymbol{T}^{(i)}_{4m} \vdots \boldsymbol{L}_4, \qquad m = 0, 2, 4, \tag{A 11}$$

which follow from (8.5), (A 5) and (A 6).

By inserting (8.4) and (8.5) into (A 10) and (A 11), and evaluation of the scalar products, evolution (5.3) are obtained, with

$$d_{11} = \frac{1}{2\sqrt{6}}a_2, \tag{A 12}$$

$$d_{12} = -\frac{1}{6}\sqrt{\frac{5}{6\pi}}(3a_5 + a_7), \tag{A 13}$$

$$-\frac{70\sqrt{2}}{3}d_{13} = -20\sqrt{\frac{7}{3}}d_{22} = -140\sqrt{\frac{10}{3}}d_{36} = 20\sqrt{\frac{7}{3}}d_{37} = a_8, \tag{A 14}$$

$$d_{21} = -\frac{1}{2}\sqrt{\frac{5}{6\pi}}(6 + a_5), \tag{A 15}$$

$$d_{31} = -\sqrt{\frac{6\pi}{5}}a_0, \tag{A 16}$$

$$d_{32} = -\frac{1}{24}\sqrt{\frac{5}{6\pi}}(6a_4 + a_7), \tag{A 17}$$

$$d_{33} = -\frac{1}{4}\sqrt{\frac{5}{6\pi}}(-12 + 2a_4 + a_7), \tag{A 18}$$

$$d_{34} = -\frac{1}{4}\sqrt{\frac{5}{6\pi}}(2a_4 + 2a_5 + a_7), \tag{A 19}$$

$$-\sqrt{\frac{35}{2}}d_{41} = -\sqrt{\frac{14}{3}}d_{61} = d_{71} = 5\sqrt{21}b_1, \tag{A 20}$$

$$d_{42} = \frac{5}{6\sqrt{6\pi}}(7b_4 + 2b_5), \tag{A 21}$$

$$\frac{1}{3}\sqrt{\frac{7}{10}}d_{43} = d_{52} = \frac{1}{3}\sqrt{\frac{14}{3}}d_{65} = -d_{73} = \frac{1}{4\sqrt{7}}b_3, \tag{A 22}$$

$$d_{51} = \frac{5}{6}\sqrt{\frac{5}{2\pi}}b_4, \tag{A 23}$$

$$d_{62} = \frac{5}{12}\sqrt{\frac{5}{2\pi}}(b_4 - b_5), \tag{A 24}$$

$$d_{63} = \frac{5}{6}\sqrt{\frac{5}{2\pi}}b_5, \tag{A 25}$$

$$d_{64} = \frac{5}{6}\sqrt{\frac{5}{2\pi}}(b_4 + b_5), \tag{A 26}$$

$$d_{72} = -\frac{5}{12}\sqrt{\frac{35}{3\pi}}(b_4 + 2b_5), \tag{A 27}$$

and

$$D_1 = a_1, \tag{A 28}$$

$$D_2 = \frac{1}{12}\sqrt{\frac{5}{\pi}}a_3, \tag{A 29}$$

$$D_3 = b_0, \tag{A 30}$$

$$D_4 = \sqrt{\frac{1}{15}}D_{41} = \sqrt{\frac{2}{35}}D_{42} = 5\pi^{-1/2}b_2. \tag{A 31}$$

Appendix B. Spherical harmonics

B.1. *Definitions of tensor spherical harmonics*

For the sake of completeness, we list the definitions of scalar- and vector-spherical harmonics (Jones 1985; Varshalovich *et al.* 1988). The vector-spherical harmonics are defined as

$$\left.\begin{aligned} \boldsymbol{y}_{jm0} &= [j(j+1)]^{-1/2} r\tilde{\nabla}\mathbf{Y}_{jm}, \\ \boldsymbol{y}_{jm1} &= -\mathrm{i}\hat{\boldsymbol{r}} \times \boldsymbol{y}_{jm0}, \\ \boldsymbol{y}_{jm2} &= \hat{\boldsymbol{r}}\mathbf{Y}_{jm}, \end{aligned}\right\} \tag{B 1}$$

where $\tilde{\nabla}$ denotes the angular part of the gradient operator. The vectors $\boldsymbol{y}_{jm0}$ and $\boldsymbol{y}_{jm1}$ are tangential, while $\boldsymbol{y}_{jm2}$ is normal to a sphere.

The tensor spherical harmonics are defined as

$$\left.\begin{aligned} \mathbf{Y}_{jj-2m} &= r^{2-j}\left[\frac{j+1}{(j-1)(2j-1)(2j+1)}\right]^{1/2}\nabla'\left(r^{j-1}\left(\boldsymbol{y}_{jm0} + \left[\frac{j}{j+1}\right]^{1/2}\boldsymbol{y}_{jm2}\right)\right) \\ \mathbf{Y}_{jj-1m} &= r^{1-j}\left[\tfrac{1}{2}(j-1)(2j+1)\right]^{-1/2}\nabla'(r^j\,\boldsymbol{y}_{jm1}) \end{aligned}\right\} \tag{B 2}$$

and

$$\left.\begin{aligned}
\mathbf{Y}_{jjm} &= r^{-j}\left[\frac{6}{(2j+3)(2j-1)}\right]^{1/2}\boldsymbol{\nabla}'\left(r^{j+1}\left(\boldsymbol{y}_{jm0}-\left[\frac{j+1}{j}\right]^{1/2}\boldsymbol{y}_{jm2}\right)\right),\\
\mathbf{Y}_{jj+1m} &= r^{2+j}\left[\tfrac{1}{2}(2-j)(2j+1)\right]^{-1/2}\boldsymbol{\nabla}'\left(r^{-j-1}\boldsymbol{y}_{jm1}\right),\\
\mathbf{Y}_{jj+2m} &= r^{3+j}\left[\frac{j}{(j+2)(2j+3)(2j+1)}\right]^{1/2}\boldsymbol{\nabla}'\left(r^{-j-2}\left(\boldsymbol{y}_{jm0}-\left[\frac{j+1}{j}\right]^{1/2}\boldsymbol{y}_{jm2}\right)\right),
\end{aligned}\right\} \tag{B 3}$$

where $\boldsymbol{\nabla}'$ denotes taking a symmetric, traceless gradient of a vector harmonic. The spherical tensor basis $\boldsymbol{a}_{2m}$ discussed in Bławzdziewicz *et al.* (2000) corresponds to $\mathbf{Y}_{20m}$.

B.2. *Rate-of-strain tensor*

The basic set of solution $\boldsymbol{u}^{\pm}_{jmq}$ (4.14) is introduced in Bławzdziewicz *et al.* (2000). Taking a symmetric, traceless gradient of a vector harmonic of order j produces five tensorial harmonics with an angular number l taking values $j-2,\ j-1,\ j,\ j+1,\ j+2$ (Varshalovich *et al.* 1988). Here we list the rate-of-strain matrices defined as $\boldsymbol{\nabla}'\boldsymbol{u}^{\pm}_{jmq} = \mathscr{U}^{\pm}_{qq'}\mathbf{Y}_{jj+q'm}$:

$$\mathscr{U}^{+}_{qq'}(j;r) = r^{j}\begin{pmatrix} A^{+}_{0-2}(r^{-2}+B^{+}_{0-2}) & 0 & A_{00}\ 0\ 0\\ 0 & A^{+}_{1-1}r^{-1} & 0\ \ 0\ 0\\ A^{+}_{2-2}(r^{-2}+B^{+}_{2-2}) & 0 & A^{+}_{20}\ 0\ 0\end{pmatrix} \tag{B 4}$$

and

$$\mathscr{U}^{-}_{qq'}(j;r) = r^{-j-1}\begin{pmatrix} 0\ 0\ A^{-}_{00} & 0 & A^{-}_{02}(r^{-2}+B^{-}_{02})\\ 0\ 0\ \ 0 & A^{-}_{11}r^{-1} & 0\\ 0\ 0\ A^{-}_{20} & 0 & A^{-}_{22}(r^{-2}+B^{-}_{22})\end{pmatrix}, \tag{B 5}$$

where

$$\left.\begin{aligned}
&A^{+}_{0-2} = -\tfrac{1}{2}\left[(-1+j)(1+j)(1+2j)(-1+2j)\right]^{1/2}, \quad B^{+}_{0-2} = \frac{3+2j}{1-2j},\\
&A^{+}_{00} = -\left[\frac{3(3+2j)}{2(-1+2j)}\right]^{1/2},\\
&A^{+}_{1-1} = \left[\tfrac{1}{2}(-1+j)(1+2j)\right]^{1/2},\\
&A^{+}_{2-2} = -\tfrac{1}{2}\left[\frac{(-1+j)(1+2j)}{j(-1+2j)}\right]^{1/2}(j(5+2j)-3), \quad B^{+}_{2-2} = \frac{j(5+2j)+3}{j(5+2j)-3},\\
&A^{+}_{20} = \left[\frac{3(1+j)(3+2j)}{2j(-1+2j)}\right]^{1/2},
\end{aligned}\right\} \tag{B 6}$$

and

$$\left.\begin{aligned}
A^{-}_{00} &= \left[\frac{3\,(2j-1)}{2\,(2j+3)}\right]^{1/2},\\
A^{-}_{02} &= \frac{1}{2}\,[j\,(j+2)\,(2j+1)\,(2j+3)]^{1/2}, \quad B^{-}_{02} = \frac{1-2j}{2j+3},\\
A^{-}_{11} &= \left[\frac{1}{2}\,(j+2)\,(2j+1)\right]^{1/2},\\
A^{-}_{20} &= \left[\frac{3j\,(2j-1)}{2\,(j+1)\,(2j+3)}\right]^{1/2},\\
A^{-}_{22} &= -\frac{1}{2}\left[\frac{(j+2)\,(2j+1)}{(j+1)\,(2j+3)}\right]^{1/2}(6-j\,(2j-1)), \quad B^{-}_{22} = \frac{6+j\,(2j-1)}{6-j\,(2j-1)}.
\end{aligned}\right\} \tag{B 7}$$

B.3. *Recoupling formulae for products of vector- and tensor-spherical harmonics*

Starting from the general formula for the inner product of tensor harmonics (Varshalovich *et al.* 1988) we derive new, simplified expressions for the inner product of a tensor harmonic and the tangential vector harmonic $\boldsymbol{y}_{jm0}$:

$$\boldsymbol{y}_{jm0} \cdot \boldsymbol{Y}_{j_1\, j_1+q_1\, m_1} = \boldsymbol{y}_{j_2 m_2 q_2}\,\zeta\,(j, j_1, j_2, m, m_1, m_2)\,\mathscr{C}_{q_1 q_2}\,(j, j_1, j_2), \tag{B 8}$$

where the Clebsch–Gordan coefficient ζ is defined by (B 13) and

$$\left.\begin{aligned}
\mathscr{C}_{-20} &= -\frac{(j\,(j+1)-j_2\,(j_2+1))^2 - j_1\,(2j\,(j+1)+2j_2\,(j_2+1)+j_1\,(j_1-1)\,(j_1+1))}{[j\,(j+1)\,j_1\,(j_1-1)\,(2j_1-1)\,(2j_1+1)\,j_2\,(2j_2+1)]^{1/2}},\\
\mathscr{C}_{-10} &= -c_4\,[j_1-1]^{-1/2}\left(j+j^2-j_2-j_2^2\right),\\
\mathscr{C}_{00} &= \sqrt{\frac{2}{3}}\,\frac{3\,(j\,(j+1)-j_2\,(j_2+1))^2 + j_1\,(j_1+1)\,(-4j\,(j+1)+j_1\,(j_1+1)-4j_2\,(j_2+1))}{[j\,(j+1)\,j_1\,(j_1+1)\,(2j_1-1)\,(2j_1+3)\,j_2\,(j_2+1)]^{1/2}},\\
\mathscr{C}_{10} &= -c_4\,[j_1+2]^{-1/2}\left(j+j^2-j_2-j_2^2\right),\\
\mathscr{C}_{20} &= \frac{(j\,(j+1)-j_2\,(j_2+1))^2 + (j_1+1)\,(2j\,(j+1)+2j_2\,(j_2+1)-j_1\,(j_1+1)\,(j_1+2))}{[j\,(j+1)\,(j_1+1)\,(j_1+2)\,(2j_1+1)\,(2j_1+3)\,j_2\,(2j_2+1)]^{1/2}},
\end{aligned}\right\} \tag{B 9}$$

$$\left.\begin{aligned}
\mathscr{C}_{-22} &= -2\left[\frac{j_1-1}{j\,(j+1)\,j_2\,(2j_2-1)\,(2j_2+1)}\right]^{1/2}[j\,(j+1)+j_1\,(j_1+1)-j_2\,(j_2+1)],\\
\mathscr{C}_{-12} &= c_4\,[(j_1-1)\,j_2\,(j_2+1)]^{1/2},\\
\mathscr{C}_{02} &= \sqrt{6}\,\frac{j\,(j+1)+(j_1-j_2)\,(j_1+j_2+1)}{[j\,(j+1)\,j_1\,(j_1+1)\,(2j_1-1)\,(2j_1+3)]^{1/2}},\\
\mathscr{C}_{22} &= 2\left[\frac{j_1+2}{j\,(j+1)\,(j_1+1)\,(2j_1+1)\,(2j_1+3)}\right]^{1/2}[j\,(j+1)+j_1\,(j_1+1)-j_2\,(j_2+1)],\\
\mathscr{C}_{12} &= -c_4\,[(j_1+2)\,j_2\,(j_2+1)]^{1/2}
\end{aligned}\right\} \tag{B 10}$$

$$\left.\begin{aligned}
\mathscr{C}_{-21} &= -c_2\left(j + j^2 - j_1 + j_1^2 - j_2 - j_2^2\right)\left[j_1\left(j_1-1\right)\left(2\,j_1-1\right)\right]^{-1/2},\\
\mathscr{C}_{-11} &= c_3\left[j_1-1\right]^{-1/2},\\
\mathscr{C}_{01} &= -2c_2\left(3j + 3j^2 - j_1 - j_1^2 - 3j_2 - 3j_2^2\right)\left[\frac{2j_1+1}{6j_1\left(j_1+1\right)\left(2\,j_1-1\right)\left(2\,j_1+3\right)}\right]^{1/2},\\
\mathscr{C}_{11} &= c_3\left[j_1+2\right]^{-1/2},\\
\mathscr{C}_{21} &= -c_2\left(2 + j + j^2 + 3j_1 + j_1^2 - j_2 - j_2^2\right)\left[\left(j_1+1\right)\left(j_1+2\right)\left(2\,j_1+3\right)\right]^{-1/2}.
\end{aligned}\right\} \tag{B 11}$$

In the above expressions

$$\left.\begin{aligned}
c_2 &= \left[\frac{\left(j+j_1-j_2\right)\left(j-j_1+j_2\right)\left(-j+j_1+j_2+1\right)\left(j+j_1+j_2+1\right)}{j\left(j+1\right)j_2\left(j_2+1\right)\left(2j_1+1\right)}\right]^{1/2},\\
c_3 &= \left[2\left(2j+1\right)\left(2j_2+1\right)\right]^{1/2}\left[j\left(j+1\right)j_1\left(j_1+1\right)j_2\left(j_2+1\right)\right]^{-1/2}\\
&\quad\times\left(j_2\left(1+j_2\right)\left(j+j^2+j_1+{j_1}^2-j_2-j_2^2\right)\right.\\
&\quad\left.+\,j\left(1+j\right)\left(-j-j^2+j_1+j_1^2+j_2^2\right)\right),\\
c_4 &= \left[\frac{\left(2j+1\right)\left(2j_2+1\right)\left(j+j_1-j_2\right)\left(j-j_1+j_2\right)\left(1-j+j_1+j_2\right)\left(1+j+j_1+j_2\right)}{j\left(j+1\right)j_1\left(j_1+1\right)j_2\left(j_2+1\right)}\right]^{1/2}.
\end{aligned}\right\} \tag{B 12}$$

B.4. *Clebsch–Gordan coefficient*

For the sake of completeness, we list the definition of the Clebsch–Gordan coefficient

$$\zeta\left(j, j_1, j_2, m, m_1, m_2, q+q_2\right) = \frac{(-1)^{m_2}}{2}\left[\frac{(2j+1)(2j_1+1)(2j_2+1)}{4\pi}\right]^{1/2} \times \begin{pmatrix} j-\xi & j_1 & j_2\\ 0 & 0 & 0\end{pmatrix}\begin{pmatrix} j & j_1 & j_2\\ m & m_1 & -m_2\end{pmatrix}, \tag{B 13}$$

where $\xi = 1$ if $q+q_2$ is even (or zero) and $\xi = 0$ if $q+q_2$ is odd.

$$\begin{pmatrix} j & j_1 & j_2\\ m & m_1 & m_2\end{pmatrix}$$

is the Wigner $3j$-symbol (Edmonds (1960)). More details about the definition and properties of ζ can be found in Bławzdziewicz *et al.* (2000). The functions χ and θ, which appear in the recoupling formulae for products of spherical harmonics (Vlahovska *et al.* 2005), are defined as

$$\chi(j, j_1, j_2) = j\left(j+1\right) + j_2\left(j_2+1\right) - j_1\left(j_1+1\right), \tag{B 14}$$

$$\theta\left(j, j_1, j_2\right) = \left[\left(j+j_1-j_2\right)\left(j-j_1+j_2\right)\left(1-j+j_1+j_2\right)\left(1+j+j_1+j_2\right)\right]^{1/2}. \tag{B 15}$$

Appendix C. Evaluation of quantities on the interface of the deformed drop

C.1. *Surface velocity*

Section 4.3.1 outlined the matrix representation of the surface velocity. The kth term in the Taylor series expansion of the velocity contains the product of k shape parameters

f^k. It is recoupled as

$$f^k = \Phi^{(k)}_{lm_l}(\boldsymbol{f}) Y_{lm_l}. \tag{C 1}$$

The coefficient $\Phi^{(k)}_{lm_l}(\boldsymbol{f})$ is evaluated by the following recursive formula (Vlahovska *et al.* 2005):

$$\Phi^{(k)}_{jm} = 2 \sum_{j_1=0}^{(k-1)j_{max}} \sum_{m_1=-j_1}^{j_1} \Phi^{(k-1)}_{j_1 m_1} \sum_{j_2=2}^{j_{max}} \sum_{m_2=-j_2}^{j_2} f_{j_2 m_2} \zeta\,(j_1, j_2, j, m_1, m_2, m, 4), \tag{C 2}$$

where

$$\Phi^{(2)}_{jm} = 2 \sum_{j_1=2}^{j_{max}} \sum_{j_2=2}^{j_{max}} \sum_{m_1=-j_1}^{j_1} \sum_{m_2=-j_2}^{j_2} f_{j_1 m_1} f_{j_2 m_2} \zeta\,(j_1, j_2, j, m_1, m_2, m, 4). \tag{C 3}$$

After recoupling the product $Y_{lm_l} \boldsymbol{y}_{jmq_1}$ (Vlahovska *et al.* 2005), we can write for the expansion terms in (4.22)

$$U^{\pm,(k)}_{qq_1}(j; r=1)\, \boldsymbol{y}_{jmq_1} = \boldsymbol{D}^{\pm}_{jmqj_2m_2q_2,k}(\boldsymbol{f})\, \boldsymbol{y}_{j_2m_2q_2}, \tag{C 4}$$

where

$$\boldsymbol{D}^{\pm}_{jmqj_2m_2q_2,k} = \sum_{l=0}^{k\, j_{max}} \sum_{m_l=-l}^{l} \Phi_{lm_l,k} \zeta\,(j\, l\, j_2\, m\, m_l\, m_2, q+q_1)\, U^{\pm,(k)}_{qq_1}(j)\, C_{q_1q_2}(jlj_2). \tag{C 5}$$

Here we list only the matrices $\boldsymbol{D}^{\pm}_k$ for $k=1$; the expressions for order 2 are rather lengthy and can be found in Vlahovska (2003):

$$\boldsymbol{D}^{+}_{jmqj_2m_2q_2,1} = \sum_{l\, m_l} f_{l\, m_l} \zeta\,(j, l, j_2, m, m_l, m_2, q+q_2)$$
$$\times \begin{pmatrix} 2\left[\dfrac{(j+1)}{j\, j_2\,(j_2+1)}\right]^{1/2} \chi\,(j,l,j_2) & -2\left[\dfrac{(j+1)}{j\, j_2\,(j_2+1)}\right]^{1/2} \theta\,(j,l,j_2) & 2\,[j\,(j+1)]^{1/2} \\ -\left[\dfrac{j}{(j+1)\, j_2\,(j_2+1)}\right]^{1/2} \theta\,(j,l,j_2) & \left[\dfrac{j}{(j+1)\, j_2\,(j_2+1)}\right]^{1/2} \chi\,(j,l,j_2) & 0 \\ -\dfrac{3+j}{j}\,[j_2\,(j_2+1)]^{-1/2}\,\chi\,(j,l,j_2) & \dfrac{3+j}{j}\,[j_2\,(j_2+1)]^{-1/2}\,\theta\,(j,l,j_2) & -4 \end{pmatrix} \tag{C 6}$$

$$\boldsymbol{D}^{-}_{jmqj_2m_2q_2,1} = \sum_{l\, m_l} f_{l\, m_l} \zeta\,(j, l, j_2, m, m_l, m_2, q+q_2)$$
$$\times \begin{pmatrix} -2\left[\dfrac{j}{(j+1)\, j_2\,(j_2+1)}\right]^{1/2} \chi\,(j,l,j_2) & \left[\dfrac{(j+1)}{j\, j_2\,(j_2+1)\, j}\right]^{1/2} \theta\,(j,l,j_2) & 2\,[j\,(j+1)]^{1/2} \\ 2\left[\dfrac{j}{(j+1)\, j_2\,(j_2+1)}\right]^{1/2} \theta\,(j,l,j_2) & -\left[\dfrac{(j+1)}{j\, j_2\,(j_2+1)\, j}\right]^{1/2} \chi\,(j,l,j_2) & 0 \\ -\dfrac{-2+j}{j+1}\,[j_2\,(j_2+1)]^{-1/2}\,\chi\,(j,l,j_2) & \dfrac{-2+j}{j+1}\,[j_2\,(j_2+1)]^{-1/2}\,\theta\,(j,l,j_2) & -4 \end{pmatrix}. \tag{C 7}$$

C.2. *Hydrodynamic tractions*

The first term in the expression for the surface tractions (4.7) corresponds to tractions on a sphere

$$\hat{\boldsymbol{r}}\cdot\bar{\boldsymbol{T}}_p=\sum_{k=0}^{p}c^{\pm}_{jmq,p-k}\boldsymbol{R}^{\pm,(k)}_{qq_1}(j)\,\boldsymbol{y}_{j_2m_2q_2}, \tag{C 8}$$

where the matrix $R^{\pm}_{qq_1}$ is defined as

$$\hat{\boldsymbol{r}}\cdot\boldsymbol{T}^{\pm}_{jmq}(\boldsymbol{r})=\boldsymbol{R}^{\pm}_{qq_1}(j;r)\,\boldsymbol{y}_{jmq_1}, \tag{C 9}$$

and the superscript, (k) denotes the kth term in the Taylor series. When evaluating the tractions on a sphere (C 8) we avoid the direct coupling of a vector and tensor harmonics by using the relation

$$\hat{\boldsymbol{r}}\cdot\nabla'\boldsymbol{u}=r\frac{\mathrm{d}}{\mathrm{d}r}\left(\frac{\boldsymbol{u}}{r}\right)+\frac{1}{r}\nabla(\boldsymbol{u}\cdot\boldsymbol{r}). \tag{C 10}$$

Inserting (4.14) in (C 10) yields

$$\left.\begin{aligned}
\boldsymbol{R}^{\pm}_{q0}(j;r)&=r\frac{\mathrm{d}}{\mathrm{d}r}\left(\frac{U^{\pm}_{0q}(j;r)}{r}\right)+[j(j+1)]^{1/2}\frac{U^{\pm}_{2q}}{r},\\
\boldsymbol{R}^{\pm}_{q1}(j;r)&=r\frac{\mathrm{d}}{\mathrm{d}r}\left(\frac{U^{\pm}_{1q}(j;r)}{r}\right), \qquad q=0,1,2,\\
\boldsymbol{R}^{\pm}_{q2}(j;r)&=-P^{\pm}_{q}(j;r)+2\frac{\mathrm{d}}{\mathrm{d}r}U^{\pm}_{2q}(j;r).
\end{aligned}\right\} \tag{C 11}$$

At leading order $k=0$ (4.28), the drop is not yet deformed and the surface tractions are evaluated on sphere

$$\Theta_{qq'}(j)=\boldsymbol{R}^{\pm}_{qq'}(j;1). \tag{C 12}$$

Hence,

$$\Theta^{+}_{qq'}(j)=\begin{pmatrix} 2j+1 & 0 & -3\left(\dfrac{j+1}{j}\right)^{1/2}\\ 0 & j-1 & 0\\ -3\left(\dfrac{j+1}{j}\right)^{1/2} & 0 & 2j+1+\dfrac{3}{j}\end{pmatrix}, \tag{C 13}$$

$$\Theta^{-}_{qq'}(j)=\begin{pmatrix} -2j-1 & 0 & 3\left(\dfrac{j}{j+1}\right)^{1/2}\\ 0 & -j-2 & 0\\ 3\left(\dfrac{j}{j+1}\right)^{1/2} & 0 & -2j-1-\dfrac{3}{j+1}\end{pmatrix}. \tag{C 14}$$

The subsequent perturbations require the evaluation of the term

$$\boldsymbol{n}_{p-k}\cdot\boldsymbol{T}_k=\boldsymbol{n}_{p-k}\cdot\nabla'\boldsymbol{u}^{\pm}_k-p^{\pm}_k\boldsymbol{n}_{p-k}. \tag{C 15}$$

The expansion of the normal vector (4.8), however, contains not only radial but also tangential vector harmonics. A simplification similar to (C 10) is unavailable for the product of tangential vector harmonic and tensor harmonic. Hence, it has to be

evaluated using the relations in (B.3). The $k = 1$ term in (4.27) has a general form

$$\Theta^{\pm}_{jmqj_2m_2q_2,1} = \sum_{lm_l} \zeta\,(j\,l\,j_2\,m\,m_l\,m_2\,q + q_2)\,f_{l\,m_l}\Big[\boldsymbol{R}^{\pm,(1)}_{qq_1}(j)\,C_{q_1q_2}(j,l,j_2)$$
$$-\,[l\,(l+1)]^{1/2}\,\mathscr{U}^{\pm}_{qq_1}(j)\,\mathscr{C}_{q_1q_2}(l,j_1,j_2) + [l\,(l+1)]^{1/2}\,P^{\pm}_{q}(j)\,C_{2q_2}(l,j,j_2)\Big]. \quad \text{(C 16)}$$

After some algebra, it is reduced to

$$\Theta^{\pm}_{jmqj_2m_2q_2,1} = \sum_{lm_l} f_{lm_l}\zeta\,(j\,l\,j_2\,m\,m_l\,m_2\,q + q_2)\,[j\,(j+1)\,j_2\,(j_2+1)]^{-1/2}\,X^{1,\pm}_{qq_2}(j,l,j_2)\,, \quad \text{(C 17)}$$

where

$$\left.\begin{aligned} X^{1,-}_{00} &= \chi(j,l,j_2)(-\chi(j,j_2,l)+1+7j+4j^2) + j(2j-1)\chi\,(l,j,j_2)\,,\\ X^{1,-}_{01} &= -1-6j-\chi\,(j,l,j_2)\,,\\ X^{1,-}_{02} &= [j_2\,(j_2+1)]^{1/2}\,(-12j\,(j_+1) - (2j+1)\,\chi\,(j,l,j_2))\,, \end{aligned}\right\} \quad \text{(C 18)}$$

$$\left.\begin{aligned} X^{1,-}_{10} &= -4-3j-\chi\,(j,l,j_2)\,,\\ X^{1,-}_{12} &= [j_2\,(j_2+1)]^{1/2}\,(2+j)\,, \end{aligned}\right\} \quad \text{(C 19)}$$

$$\left.\begin{aligned} X^{1,-}_{20} &= (j+1)^{-1}[j(j+1)]^{1/2}(-2j_2(j_2+1)(2+3j-2j^2) - 9\chi(j,l,j_2)),\\ X^{1,-}_{21} &= \frac{9}{1+j}\,[j\,(j+1)]^{1/2},\\ X^{1,-}_{22} &= \frac{3}{1+j}\,[j\,(j+1)\,j_2\,(j_2+1)]^{-1/2}\,(-8\,(j+1) + \chi\,(j,l,j_2)), \end{aligned}\right\} \quad \text{(C 20)}$$

and

$$\left.\begin{aligned} X^{1,+}_{00} &= \chi\,(j,l,j_2)^2 - (5+6j)\,\chi\,(j,l,j_2) + 2j_2\,(j_2+1)\,(3+5j+2j^2),\\ X^{1,+}_{01} &= 5+6j-\chi\,(j,l,j_2)\,,\\ X^{1,+}_{02} &= [j_2\,(j_2+1)]^{1/2}\,(-12j\,(1+j) + (2j+1)\,\chi\,(j,l,j_2))\,, \end{aligned}\right\} \quad \text{(C 21)}$$

$$\left.\begin{aligned} X^{1,+}_{10} &= -1+3j-\chi\,(j,l,j_2)\,,\\ X^{1,+}_{12} &= [j_2\,(j_2+1)]^{1/2}\,(1-j)\,, \end{aligned}\right\} \quad \text{(C 22)}$$

$$\left.\begin{aligned} X^{1,+}_{20} &= [j\,(j+1)]^{1/2}\,j^{-1}\left(-2j_2\,(j_2+1)\left(3+7j+2l^2\right) + 9\chi\,(j,l,j_2)\right),\\ X^{1,+}_{21} &= -\frac{9}{j}\,[j\,(j+1)]^{1/2},\\ X^{1,+}_{22} &= -\frac{3}{j}\,[j\,(j+1)\,j_2\,(j_2+1)]^{1/2}\,(-8j + \chi\,(j,l,j_2)). \end{aligned}\right\} \quad \text{(C 23)}$$

For $k = 2$, the explicit expressions become very cumbersome and can be found in Vlahovska (2003).

C.3. *Recurrence relations for the velocity*

The expressions for $\Theta^{\pm}_{qq'}$ are used to find $\Upsilon_{qq'}$ (4.33). Thus, (4.31) becomes

$$\left.\begin{aligned} c^{-}_{jm2,p} &= d(j)d(j_1)[-3z_{jm0,p}(-1+\chi(j+1))+z_{jm2,p}\,j\,(j+1)\,(1+2j)\chi],\\ c^{-}_{jm1,p} &= -d_c(j)d(j_1)z_{jm1,p},\\ c^{-}_{jm0,p} &= d(j)d(j_1)[z_{jm0,p}[j\,(j+1)]^{1/2}(3-(j+1)(3+j+j^2)\chi)\\ &\quad -3z_{jm2,p}\,[j\,(j+1)]^{1/2}\,(-1+\chi(j+1))], \end{aligned}\right\} \tag{C 24}$$

where z was defined by (4.32), $d\,(j)$ by (D 11) and $d_c\,(j)$ by (D 15).

C.4. *Evolution equation matrices*

The two terms in (3.4) describe interface evolution due to fluid motion radial and tangential to a sphere (the expansion of ∇f involves only tangential vector-spherical harmonics),

$$\boldsymbol{u}_s\cdot\hat{\boldsymbol{r}}=\sum_{p=0}\varepsilon^p\varrho_{jm,p}Y_{jm}, \tag{C 25}$$

$$\varepsilon\boldsymbol{u}_s\cdot\nabla f=\sum_{p=1}\varepsilon^p\vartheta_{jm,p}Y_{jm}. \tag{C 26}$$

Radial and tangential vector harmonics do not couple (Bławzdziewicz *et al.* 2000; Vlahovska *et al.* 2005), and in particular $\hat{\boldsymbol{r}}\cdot\boldsymbol{y}_{jmq}=\delta_{q2}Y_{jm}$. Hence, in the product of the surface velocity (4.23) and the unit radial vector only matrix coefficients $\boldsymbol{D}^{\pm}_{j'm'q'jmq,k}$ with $q=2$ remain

$$\varrho_{jm,p}=c^{\pm}_{jm2,p}+\sum_{k=1}^{p}c^{\pm}_{j'm'q',p-k}\boldsymbol{D}^{\pm}_{j'm'q'jm2,k}\,(\boldsymbol{f})\quad \nu=in,\ \text{out}, \tag{C 27}$$

where the diagonal form of $\boldsymbol{D}^{\pm}_{j'm'q'jm2,0}$ (4.24) is taken into account. For the second term (C 26), we get

$$\vartheta_{jm,p}Y_{jm}=\sum_{k=1}^{p}\sum_{n=0}^{p-k}c^{\pm}_{j'''m'''q''',p-k-n}\boldsymbol{D}^{\pm}_{j'''m'''q'''j'm'q',n}(\boldsymbol{f})\boldsymbol{N}_{j''m''q'',k}\,(\boldsymbol{f})\,\boldsymbol{y}_{j'm'q'}\cdot\boldsymbol{y}_{j''m''q''}, \tag{C 28}$$

where the matrix $\boldsymbol{N}$ is the spherical harmonics representation of ∇f, given in Vlahovska *et al.* (2005).

The scalar product of vector harmonics in (C 28) is further recoupled using the formulae from Bławzdziewicz *et al.* (2000) and Vlahovska *et al.* (2005). Combining (C 27) and (C 28) yields

$$\begin{aligned}\boldsymbol{W}^{\pm,F}_{jmqj_2m_2,k}&=\boldsymbol{D}^{\pm}_{jmqj_2m_22,k}\\ &\quad+\sum_{n=1}^{k}\boldsymbol{D}^{\pm}_{jmqj'm'q',k-n}\boldsymbol{N}_{j''m''q'',n}C_{q'q''}(j'\,j''\,j_2)\zeta(j'\;j''\;j_2\,m'\,m''\,m_2,q'+q''),\end{aligned} \tag{C 29}$$

where $\boldsymbol{N}_{jmq,n}$ represents the nth term in the expansion of ∇f.

The surfactant evolution (3.6) requires evaluation of the divergence of the product of angular velocity and surfactant distribution. At the deformed interface, the tangential

angular velocity introduced by (3.7) is expanded as

$$\tilde{\boldsymbol{u}}(\boldsymbol{r}_s) = \sum_{p=0} \varepsilon^p \tilde{\boldsymbol{u}}_p(\Omega). \tag{C 30}$$

Inserting the surface velocity expansion (4.23) and expanding r_s^{-1} in the Taylor series, we obtain

$$\tilde{\boldsymbol{u}}_p(\Omega) = \left(c^{\pm}_{jmq,p} + \sum_{k=1}^{p} c^{\pm}_{j'm'q',p-k} A^{\pm}_{j'm'q'jmq,k}(\boldsymbol{f}) \right) \boldsymbol{y}_{jmq}, \quad q = 0, 1, \tag{C 31}$$

where

$$A^{\pm}_{jmqj_2m_2q_2,k} = \sum_{l=0}^{k\, j_{max}} \sum_{m_l=-l}^{l} \Phi_{lm_l,k} \zeta(j\, l\, j_2\, m\, m_l\, m_2, q + q_1) C_{q_1q_2}(jlj_2) \sum_{n=0}^{k} (-1)^k U^{\pm,(n)}_{qq_1}(j). \tag{C 32}$$

The vector–scalar harmonics couplings in the product of the angular velocity (C 31) and the surfactant concentration expansion in scalar harmonics (3.9) are recoupled according to the formulae listed in Vlahovska *et al.* (2005). Taking the divergence of the result, having in mind that the angular surface divergence of the tangential vector harmonics $\boldsymbol{y}_{jm1}$ is identically zero, leads to

$$W^{\pm,\Gamma}_{jmqj_2m_2,k} = D^{\pm}_{jmqj_2m_20,k} + \sum_{n=1}^{k} \sum_{j'm'j''m''} D^{\pm}_{jmqj'm'q',k-n} g_{j''m''q'',n} C_{q'q''} \times (j'j''j_2)\zeta(j'\, j''\, j_2\, m'\, m''\, m_2, q' + q''). \tag{C 33}$$

Appendix D. Perturbation solution: explicit expressions for velocity, surfactant- and shape-evolution coefficients

Because of the linearity of the Stokes equations, the fluid flow can be decomposed to a flow driven by interfacial stresses, and a disturbance flow due to a "blob" with viscosity contrast but no interfacial stresses. Accordingly, the evolution coefficients (3.8) can be split into contributions due to viscosity contrast, capillary and Marangoni stresses

$$\left.\begin{aligned} F_{jm,p} &= S^F_{jm,p} + Ca^{-1} K^F_{jm,p} + Ma\, M^F_{jm,p}, \\ G_{jm,p} &= S^\Gamma_{jm,p} + Ca^{-1} K^\Gamma_{jm,p} + Ma\, M^\Gamma_{jm,p}. \end{aligned}\right\} \tag{D 1}$$

In the following subsections, explicit expressions for velocity, shape and surfactant evolution coefficients for the perturbation order 1 are listed. The expressions for orders 2 and 3 are very cumbersome and can be found in Vlahovska (2003).

D.1. *Leading-order perturbation solution*

The leading-order solution describes the distorting effect on shape and surfactant distribution by the extensional component of the external flow.

The linear flow (4.20) can be decomposed into pure straining

$$c^{\infty}_{2m0} = \mathrm{s}\sqrt{\frac{\pi}{5}}, \quad c^{\infty}_{2m2} = \mathrm{s}\sqrt{\frac{2\pi}{15}}, \tag{D 2}$$

and rigid body rotation

$$c^{\infty}_{101} = \omega \mathrm{i}\sqrt{\frac{2\pi}{3}}. \tag{D 3}$$

Irrotational flows are characterized by $\omega = 0$. The axisymmetric extensional flow $\boldsymbol{u}^{\infty} = (-1/2x, -1/2y, z)$ is specified by $\mathrm{s} = \sqrt{6}$ and $m = 0$. Simple shear flow $\boldsymbol{u}^{\infty} = (y, 0, 0)$ is given by $\omega = 1$, $m = \pm 2$ and $\mathrm{s} = -\,\mathrm{sign}(m)\mathrm{i}$. Hyperbolic flow $\boldsymbol{u}^{\infty} = (x, -y, 0)$ is given by $m = \pm 2$ and $\mathrm{s} = 2$.

The straining part of the external flow stretches the drop along the extensional axis and convects the surfactant towards drop tips. These processes are described by the leading-order terms, $p = 0$, in the evolution equation for shape and surfactant; accordingly, the terms corresponding to relaxation driven by capillary $K_{jm,0}$ and Marangoni stresses $M_{jm,0}$ are zero. The extensional part of the imposed flow (D 2) is described by $j = 2$ harmonics, and thus only $j = 2$ harmonics are excited in the disturbance flow field. After solving (4.31), taking into account (D 2) and (D 3) for the expansion coefficients for the velocity and stress fields, we obtain

$$\begin{aligned} c^{+}_{2m0,0} &= c^{-}_{2m0,0} + c^{\infty}_{2m0,0} = \frac{\mathrm{s}}{1+2\chi}\sqrt{5\pi} \\ c^{+}_{2m2,0} &= c^{-}_{2m2,0} + c^{\infty}_{2m2,0} = \frac{\mathrm{s}}{1+2\chi}\sqrt{\frac{10\pi}{3}} \\ c^{+}_{101,0} &= c^{-}_{101,0} + c^{\infty}_{101,0} = \omega \mathrm{i}\sqrt{\frac{2\,\pi}{3}}. \end{aligned} \tag{D 4}$$

The only non-zero terms in the evolution (D 1) are

$$S^{F}_{2m,0} = \frac{\mathrm{s}}{1+2\chi}\sqrt{\frac{10\pi}{3}}, \qquad S^{\Gamma}_{2m,0} = \mathrm{s}\frac{\sqrt{30\pi}}{1+2\chi}. \tag{D 5}$$

D.2. *Order 1 perturbation solution*

The order $p = 1$ solution describes the flow due to the deformed drop, i.e. the restoring effect of interfacial stresses and drop rotation. The expressions are given in a general form that can be applied for any external flow.

D.2.1. *Velocity field generated by interfacial stresses*

Capillary and Marangoni stresses drive fluid flow that opposes the shape and surfactant distortion induced the external flow. At this order, capillary and Marangoni velocities are continuous at the deformed interface, thus in equations (4.26), (4.38) and (4.39)

$$\left.\begin{aligned} v^{\nu}_{jmq,1} &= 0 \qquad\qquad q = 0, 1, 2 \\ w^{\pm,F,\nu}_{jm,1} &= 0,\ w^{\pm,\Gamma,\nu}_{jm,1} = 0 \quad \nu = \mathrm{cap},\ \mathrm{mar}. \end{aligned}\right\} \tag{D 6}$$

After solving (4.31) for $p = 1$, we obtain that the capillary and Marangoni terms in the velocity field are

$$\left.\begin{aligned} c^{\pm}_{jm0,1} &= -\left[j\,(j+1)\right]^{-1/2}\left(Ca^{-1}\,K^{\Gamma}_{jm,1} + Ma\,M^{\Gamma}_{jm,1}\right), \\ c^{\pm}_{jm1,1} &= 0, \\ c^{\pm}_{jm2,1} &= Ca^{-1}\,K^{F}_{jm,1} + Ma\,M^{F}_{jm,1}. \end{aligned}\right\} \tag{D 7}$$

The capillary and Marangoni terms in the evolution (D 1) are

$$\left.\begin{aligned} K^{v}_{jm,1} &= \bar{K}^{v}_{jm,1} f_{jm}, \\ M^{v}_{jm,1} &= \bar{M}^{v}_{jm,10} f_{jm} + \bar{M}^{v}_{jm,01} g_{jm}. \qquad v = F,\ \Gamma. \end{aligned}\right\} \tag{D 8}$$

For the shape-evolution equation, we have

$$\left.\begin{aligned} \bar{K}^{F}_{jm,1} &= d(j)(1-j)\,j(j+1)(j+2)(2j+1)\,\chi, \\ \bar{M}^{F}_{jm,10} &= d(j)\,j(j+1)(-6+j(j-1)(2j+5)\,\chi), \\ \bar{M}^{F}_{jm,01} &= d(j)\,j(j+1)(3+(j-1)\,\chi). \end{aligned}\right\} \tag{D 9}$$

For the surfactant evolution equation, we obtain

$$\left.\begin{aligned} \bar{K}^{\Gamma}_{jm,1} &= -d(j)3(j-1)\,j(j+1)(j+2)(-1(j+1)\,\chi), \\ \bar{M}^{\Gamma}_{jm,10} &= -d(j)j(j+1)(-3(-4+j+j^2)+(j-1)(j+1)(7j+12)\,\chi), \\ \bar{M}^{\Gamma}_{jm,01} &= d(j)j(j+1)(3+(j-1)(j+1)(2j+3)\,\chi), \end{aligned}\right\} \tag{D 10}$$

where

$$d(j) = [(3+2(j-1)(j+1)\,\chi)(-3+(3+4j+2j^2)\chi)]^{-1}. \tag{D 11}$$

D.2.2. *Velocity field due to viscosity contrast*

A 'blob' with viscosity different than the suspending fluid introduces a disturbance in the external flow. The radial component of the velocity 'jump' (4.26) for this velocity field is zero, because the first derivative of the radial velocity is continuous. However, there are tangential components due to contribution from the external flow $\boldsymbol{u}^{\infty}$:

$$\begin{aligned} v_{jm0,1} &= 2c_{\zeta 0} d(j)\,\chi(2, j_1, j), \\ v_{jm1,1} &= -c_{\zeta 1} d_c(j)\,\theta(2, j, j_1), \\ v_{jm2,1} &= 0. \end{aligned} \tag{D 12}$$

The solution for the velocity field coefficients is

$$\left.\begin{aligned} c^{-}_{jm0,1} &= c_{\zeta 0} d(j)(18(1+j)(-1+\chi(j+1))((\chi-1)\chi(2, j_1, j)+4j) \\ &\quad +\chi(2, j_1, j)(3-\chi(j+1)(3+j+2j^2)) \\ &\quad \times(\chi(2, j_1, j)+2(-2-2j+\chi(1+2j)))), \\ c^{-}_{jm1,1} &= -c_{\zeta 1} d_c(j)\,\theta(2, j_1, j)(-\chi(2, j_1, j)+2\chi(1-j)), \\ c^{-}_{jm2,1} &= 3c_{\zeta 2} d(j)\,[j(j+1)]^{1/2}\,[4+4j-\chi(2, j_1, j)](-\chi(2, j_1, j) \\ &\quad +\chi[\chi(2, j_1, j)(1+j)+2j(2j+1))], \end{aligned}\right\} \tag{D 13}$$

where

$$c_{\zeta q} = f_{j_1 m_1}\psi(j, j_1, m, m_1, q)(\chi-2)\sqrt{\frac{5}{2}}[j(j+1)]^{-1/2}[1+2\chi]^{-1}. \tag{D 14}$$

The denominator $d(j)$ is defined by (D 11) and

$$d_c(j) = [3+(j-1)\,\chi]^{-1}. \tag{D 15}$$

The functions χ and θ are defined by (B 14) and (B 15). The flow function ψ describes the coupling of the external flow, $j = 2$, and the shape modes of order j. For a simple shear flow, the flow function ψ is

$$\psi(j, j_1, m, m_1, q) = \mathrm{s}(\zeta(2, j_1, j, 2, m_1, m, q) - \zeta(2, j_1, j, -2, m_1, m, q)), \tag{D 16}$$

and for the extensional flow

$$\psi\,(j,\,j_1,\,m,\,m_1,\,q) = \mathrm{s}\zeta\,(2,\,j_1,\,j,\,2,\,0,\,0,\,0,\,q)\,, \tag{D 17}$$

where the coupling coefficient ζ is defined by (B 13). Note that if the viscosities of the drop and suspending fluid are equal, i.e. $\chi = 2$, the disturbance flow vanishes (D 14), i.e. $c^{\pm}_{jmq,1} = 0$.

We proceed next to evaluate the evolution coefficient S in (D 1). Using (D 4), we obtain from (4.38) and (4.39):

$$w^{F,+}_{jm,1} = \omega\mathrm{i}\frac{m_1}{2}\delta_{j_1 2} f_{j_1 m_1} - \sqrt{\frac{5}{2}}\frac{\psi\,(j,\,j_1,\,m,\,m_1,\,2)}{(1+2\chi)}\chi\,(1,\,j,\,j_1)\,f_{j_1 m_1}, \tag{D 18}$$

$$w^{\Gamma,+}_{jm,1} = \omega\mathrm{i}\frac{m_1}{2}\delta_{j_1 2} g_{j_1 m_1} + \sqrt{\frac{5}{2}}\frac{\psi\,(j,\,j_1,\,m,\,m_1,\,2)}{(1+2\chi)}\chi(1,\,j,\,j_1)(-f_{j_1 m_1} + g_{j_1 m_1}). \tag{D 19}$$

Combining (D 18), (D 13) and (D 12) in (4.36), we obtain for term $S_{jm,1}$ in the shape evolution

$$\begin{aligned} S^{F}_{jm,1}\,(j_1 m_1) &= \omega\mathrm{i}\frac{m_1}{2}\delta_{j_1 2} f_{j_1 m_1} \\ &\quad + f_{j_1 m_1} d\,(j)\sqrt{\frac{5}{2}}\psi\,(j,\,j_1,\,m,\,m_1,\,2)\,[(1+2\chi)]^{-1}\,(a_0 + a_1\chi + a_2\chi^2), \end{aligned} \tag{D 20}$$

where

$$\begin{aligned} a_0 = {} & -3(-1+j)(-18 + j(11 + 2(-1+j)j)) \\ & -3j_1(1+j_1)(-19 - 4(-1+j)j + 2j_1(1+j_1)) \end{aligned} \tag{D 21a}$$

$$\begin{aligned} a_1 = {} & 3(-1+j)(-26 - 7j - 3j^2 + 9^3 + 2j^4) \\ & -3j_1(1+j_1)\left(29 + 10j^2 + 4j^3 - 3j_1\,(j_1+1) - 2j\left(-9 + j_1 + j_1^2\right)\right) \end{aligned} \tag{D 21b}$$

$$\begin{aligned} a_2 = {} & (-1+j)(24 + 14j + 5j^2 + 6j^3 + 13j^4 + 4j^5) - j_1\,(j_1+1)\,(3j_1\,(j+1)\,(j_1+1) \\ & + 2(-15 + j(-16 + j(-5 + j + 2j^2)))). \end{aligned} \tag{D 21c}$$

Likewise, inserting (D 19), (D 13) and (D 12) in (4.36), we obtain for the analogous term in the surfactant evolution equation

$$\begin{aligned} S^{\Gamma}_{jm,1}\,(j_1 m_1) = {} & \omega\mathrm{i}\frac{m_1}{2}\delta_{j_1 2} g_{j_1 m_1} + \sqrt{\frac{5}{2}}\psi\,(j,\,j_1,\,m,\,m_1,\,0)\,[2\chi+1]^{-1} \\ & \times [g_{j_1 m_1}(6 + j\,(j+1) - j_1\,(j_1+1)) \\ & - f_{j_1 m_1} d\,(j)\,(-2 + j - j_1)(-1 + j + j_1)(\chi - 2)(b_0 + b_1\chi)], \end{aligned} \tag{D 22}$$

where

$$\left.\begin{aligned} b_0 &= -3(1+j)(6+j) + 3j_1(1+j_1), \\ b_1 &= (1+j)(18 + 27j + 16j^2 + 3j^3 + 2j^4) - (j+1)\,(2j^2 + j + 3)j1\,(j_1+1)\,. \end{aligned}\right\} \tag{D 23}$$

The first term on the right-hand side of equations (D 20) and (D 22) describes the rotation of the deformed drop by the rotational component of external flow (D 3).

Appendix E. Coefficients in the evolution equation

Here we list the explicit expressions for all coefficients in the evolution (5.3). The coefficients and the evolution equations can be downloaded from Vlahovska (2007).

$$c_1 = \frac{1}{2}\sqrt{\frac{15}{2\pi}}, \tag{E 1}$$

$$D_1 = -\frac{40\chi}{(2\chi+1)(19\chi-3)}, \tag{E 2}$$

$$D_2 = -\frac{24\left(137\chi^3+213\chi^2-96\chi-6\right)\sqrt{5/\pi}}{7(2\chi+1)^2(19\chi-3)^2}, \tag{E 3}$$

$$D_3 = -\frac{360\chi}{(10\chi+1)(17\chi-1)}, \tag{E 4}$$

$$D_4 = \sqrt{\frac{1}{15}}D_{41} = \sqrt{\frac{2}{35}}D_{42} = -\frac{80\chi(14\chi^2-249\chi+43)}{21(2\chi+1)(10\chi+1)(17\chi-1)(19\chi-3)\sqrt{\pi}}, \tag{E 5}$$

$$d_{11} = \frac{5(4\chi-13)}{7\sqrt{6}(2\chi+1)^2}, \tag{E 6}$$

$$d_{12} = -\frac{10(\chi-2)(13\chi-6)\sqrt{30/\pi}}{7(2\chi+1)^2(19\chi-3)}, \tag{E 7}$$

$$d_{13} = \sqrt{\frac{6}{7}}d_{22} = 2\sqrt{15}d_{36} = -\sqrt{\frac{6}{7}}d_{37} = \frac{20\sqrt{2}(43\chi^2-7\chi+17)}{7(2\chi+1)^2(19\chi-3)}, \tag{E 8}$$

$$d_{21} = -\frac{10(\chi-2)(13\chi-6)\sqrt{30/\pi}}{7(2\chi+1)^2(19\chi-3)}, \tag{E 9}$$

$$d_{31} = -\frac{\sqrt{10\pi/3}}{2\chi+1}, \tag{E 10}$$

$$d_{32} = -\frac{(2336\chi^3-22\,396\chi^2+14\,477\chi-933)\sqrt{5/6\pi}}{98(2\chi+1)^3(19\chi-3)}, \tag{E 11}$$

$$d_{33} = \frac{(2703\chi^2-647\chi+282)\sqrt{10/3\pi}}{7(2\chi+1)^2(19\chi-3)}, \tag{E 12}$$

$$d_{34} = -\frac{(13\,256\chi^3-43\,816\chi^2+11\,117\chi+4107)\sqrt{5/6\pi}}{49(2\chi+1)^3(19\chi-3)}, \tag{E 13}$$

$$d_{41} = \frac{2}{\sqrt{15}}d_{61} = -\sqrt{\frac{2}{35}}d_{71} = -\frac{\sqrt{30}}{14\chi+7}, \tag{E 14}$$

$$d_{42} = \frac{60(\chi-2)(20\chi-1)\sqrt{6/\pi}}{77(2\chi+1)^2(10\chi+1)}, \tag{E 15}$$

$$d_{43} = 3\sqrt{\frac{10}{7}}d_{52} = 2d_{65} = -3\sqrt{\frac{10}{7}}d_{73} = \frac{15\sqrt{10}(4\chi-29)}{77(20\chi^2+12\chi+1)}, \tag{E 16}$$

$$d_{51} = \frac{120(\chi-2)(29\chi-2)\sqrt{10/\pi}}{539(2\chi+1)^2(10\chi+1)}, \tag{E 17}$$

$$d_{62} = \frac{45(\chi-2)(34\chi-5)\sqrt{10/\pi}}{539(2\chi+1)^2(10\chi+1)}, \tag{E 18}$$

$$d_{63} = \frac{30(\chi-2)\sqrt{10/\pi}}{77(2\chi+1)(10\chi+1)}, \tag{E 19}$$

$$d_{64} = \frac{30(\chi-2)(130\chi-1)\sqrt{10/\pi}}{539(2\chi+1)^2(10\chi+1)}, \tag{E 20}$$

$$d_{72} = -\frac{60(\chi-2)(24\chi+1)\sqrt{15/7\pi}}{77(2\chi+1)^2(10\chi+1)}. \tag{E 21}$$

The above expressions can also be obtained from the relations in Appendix A.

$$D_{12} = \frac{12(3\chi-1)}{(2\chi+1)(19\chi-3)}, \tag{E 22}$$

$$D_{13} = \frac{2(\chi+3)}{(2\chi+1)(19\chi-3)}, \tag{E 23}$$

$$D_{21} = \frac{3(\chi+3)(918\chi^2-197\chi+47)\sqrt{5/\pi}}{7(2\chi+1)^2(19\chi-3)^2}, \tag{E 24}$$

$$D_{22} = \frac{2(181\chi^3-481\chi^2-123\chi-153)\sqrt{5/\pi}}{7(2\chi+1)^2(19\chi-3)^2}, \tag{E 25}$$

$$B_{12} = \frac{12(13\chi-1)}{(2\chi+1)(19\chi-3)}, \tag{E 26}$$

$$B_{13} = -\frac{6(7\chi+1)}{(2\chi+1)(19\chi-3)}, \tag{E 27}$$

$$B_2 = -\frac{60(12\chi^3+217\chi^2-52\chi+15)\sqrt{5/\pi}}{7(2\chi+1)^2(19\chi-3)^2}, \tag{E 28}$$

$$B_{21} = \frac{12(3\chi-1)\sqrt{5/\pi}}{7(2\chi+1)(19\chi-3)}, \tag{E 29}$$

$$B_{22} = \frac{15(446\chi^3+1277\chi^2-580\chi+9)\sqrt{5/\pi}}{7(2\chi+1)^2(19\chi-3)^2}, \tag{E 30}$$

$$B_{23} = -\frac{3(2648\chi^3+1607\chi^2-1054\chi-129)\sqrt{5/\pi}}{7(2\chi+1)^2(19\chi-3)^2}, \tag{E 31}$$

$$B_{24} = \frac{3(7\chi+1)\sqrt{5/\pi}}{7(2\chi+1)(19\chi-3)}, \tag{E 32}$$

$$b_{11} = \frac{15\sqrt{6}(\chi-2)}{7(2\chi+1)^2}, \tag{E 33}$$

$$b_{12} = \frac{5\sqrt{3/2}}{7(2\chi+1)}, \tag{E 34}$$

$$b_{13} = -\frac{30(\chi-2)(23\chi-1)\sqrt{30/\pi}}{7(2\chi+1)^2(19\chi-3)}, \tag{E 35}$$

$$b_{14} = \frac{15(\chi-2)\sqrt{15/2\pi}}{49(2\chi+1)^2}, \tag{E 36}$$

$$b_{15} = \frac{100\sqrt{2}(\chi-2)(17\chi+1)}{7(2\chi+1)^2(19\chi-3)}, \tag{E 37}$$

$$b_{16} = b_{12}4/\sqrt{3}, \qquad b_{17} = b_{15}\sqrt{7/6}, \qquad b_{18} = b_{16}\sqrt{7/6}, \tag{E 38}$$

$$b_{19} = b_{15}/2\sqrt{15} \qquad b_{20} = b_{16}/2\sqrt{15}, \tag{E 39}$$

$$b_{21} = -\frac{10(\chi-2)(2691\chi^2+751\chi-16)\sqrt{30/\pi}}{49(2\chi+1)^3(19\chi-3)}, \tag{E 40}$$

$$b_{22} = -\frac{5\sqrt{15/2\pi}}{2\chi+1}, \tag{E 41}$$

$$b_{32} = -\frac{15(\chi-2)(296\chi^2-169\chi+29)\sqrt{15/2\pi}}{49(2\chi+1)^3(19\chi-3)}, \tag{E 42}$$

$$b_{33} = \frac{5(\chi-2)(183\chi-11)\sqrt{30/\pi}}{7(2\chi+1)^2(19\chi-3)}, \tag{E 43}$$

$$b_{34} = -\frac{75(\chi-2)(188\chi^2+25\chi+3)\sqrt{30/\pi}}{49(2\chi+1)^3(19\chi-3)}. \tag{E 44}$$

$$P_{12} = \frac{40(26\chi-1)}{3(10\chi+1)(17\chi-1)}, \tag{E 45}$$

$$P_{13} = \frac{20(\chi+1)}{3(10\chi+1)(17\chi-1)}, \tag{E 46}$$

$$Q_1 = -\frac{120(5\chi-1)}{(10\chi+1)(17\chi-1)}, \tag{E 47}$$

$$Q_{12} = \frac{160(25\chi-2)}{3(10\chi+1)(17\chi-1)}, \tag{E 48}$$

$$Q_{13} = -\frac{20(55\chi+1)}{3(10\chi+1)(17\chi-1)}, \tag{E 49}$$

$$P_{21} = P_{31}/\sqrt{15} = P_{41}\sqrt{\frac{2}{35}} = -\frac{4(30\chi^3+2131\chi^2-570\chi+41)}{7(2\chi+1)(10\chi+1)(17\chi-1)(19\chi-3)\sqrt{\pi}}, \tag{E 50}$$

$$P_{22} = 2P_{32}/\sqrt{15} = P_{42}\sqrt{\frac{2}{35}} = \frac{8(140\chi^3+417\chi^2-200\chi+27)}{21(2\chi+1)(10\chi+1)(17\chi-1)(19\chi-3)\sqrt{\pi}}, \tag{E 51}$$

$$Q_2 = Q_3/\sqrt{15} = Q_4\sqrt{\frac{2}{35}} = \frac{40(2045\chi^2-376\chi+27)}{21(10\chi+1)(17\chi-1)(19\chi-3)\sqrt{\pi}}, \tag{E 52}$$

$$Q_{21} = Q_{31}/\sqrt{15} = Q_{41}\sqrt{\frac{2}{35}} = -\frac{40(1915\chi^2-424\chi+13)}{7(10\chi+1)(17\chi-1)(19\chi-3)\sqrt{\pi}}, \tag{E 53}$$

$$Q_{22} = 2Q_{32}/\sqrt{15} = Q_{42}\sqrt{\frac{2}{35}} = -\frac{40(3\chi-1)}{7(2\chi+1)(19\chi-3)\sqrt{\pi}}, \tag{E 54}$$

$$Q_{23} = 2Q_{33}/\sqrt{15} = Q_{43}\sqrt{\frac{2}{35}} = \frac{10(25\,970\chi^3 + 2589\chi^2 - 1712\chi + 33)}{21(2\chi+1)(10\chi+1)(17\chi-1)(19\chi-3)\sqrt{\pi}}, \quad \text{(E 55)}$$

$$Q_{24} = Q_{34}/\sqrt{15} = Q_{44}\sqrt{\frac{2}{35}} = -\frac{10(7\chi+1)}{7(2\chi+1)(19\chi-3)\sqrt{\pi}}, \quad \text{(E 56)}$$

$$d_{41} = \frac{3}{5}q_1 = -q_2\frac{11}{15\sqrt{3}} = -q_4 11\sqrt{\frac{2}{105}} = q_7\frac{2}{5}\sqrt{\frac{3}{5}} = -q_8\frac{22}{15\sqrt{3}}, \quad \text{(E 57)}$$

where d_{41} is given by (E 14):

$$q_3 = \frac{150\sqrt{10}(\chi-2)}{11(2\chi+1)(10\chi+1)} = q_5 3\sqrt{\frac{10}{7}} = 2q_6 = -2\sqrt{\pi}q_{12}$$
$$= -\frac{28\sqrt{\pi}}{9}q_{14} = 7\sqrt{\pi}q_{15} = -\frac{14\sqrt{\pi}}{5}q_{16} = 2\sqrt{\frac{14\pi}{3}}q_{18}, \quad \text{(E 58)}$$

$$q_9 = -b_{22}\sqrt{\frac{10\pi}{63}}, \quad \text{(E 59)}$$

$$q_{10} = -\frac{30(\chi-2)(23\chi-1)\sqrt{30/\pi}}{7(2\chi+1)^2(19\chi-3)}, \quad \text{(E 60)}$$

$$q_{11} = -\frac{15(\chi-2)\sqrt{30/\pi}}{49(2\chi+1)^2} = -\frac{\sqrt{3}}{5}q_{13} = -\frac{\sqrt{3}}{5}q_{17} = \frac{3\sqrt{\frac{2}{7}}}{5}q_{19} = -\frac{\sqrt{3}}{5}q_{13}. \quad \text{(E 61)}$$

Appendix F. Stress coefficients

The coefficients in (5.7)–(5.9) are

$$\tau_0 = \frac{5(\chi-2)}{2\chi+1}, \quad \text{(F 1)}$$

$$-\frac{7\sqrt{5\pi}}{3}\tau_{11} = -\frac{35\sqrt{\pi}}{2}\tau_{12} = \frac{1}{2}\sqrt{\frac{35\pi}{2}}\tau_{13} = \tau_0^2, \quad \text{(F 2)}$$

$$\tau_{14} = \tau_0^2\frac{9(24\chi-13)}{490(2\chi+1)\pi}, \quad \text{(F 3)}$$

$$\tau_{15} = -\tau_0^2\frac{41}{35\pi}, \quad \text{(F 4)}$$

$$\tau_{16} = \tau_0^2\frac{3(212\chi+31)}{245(2\chi+1)\pi}, \quad \text{(F 5)}$$

$$\tau_{21} = \frac{\sqrt{15/2\pi}}{2\chi+1}, \quad \text{(F 6)}$$

$$\tau_{22} = \frac{20\sqrt{6}(\chi-7)}{7(2\chi+1)^2\pi}, \quad \text{(F 7)}$$

$$\tau_{31} = -\frac{15\sqrt{6}(2\chi-29)}{14(2\chi+1)^2\pi}, \quad \text{(F 8)}$$

$$\tau_{32} = -\frac{15\sqrt{6}(\chi+3)}{14(2\chi+1)^2\pi}, \tag{F 9}$$

$$n_{11} = -\frac{4(121\chi+38)}{49(2\chi+1)\pi}\tau_0^2, \tag{F 10}$$

$$n_{21} = \frac{3\sqrt{6}}{7\pi}\tau_0^2. \tag{F 11}$$

REFERENCES

Barthès-Biesel, D. & Acrivos, A. 1973*a* Deformation and burst of a liquid droplet freely suspended in a linear shear field. *J. Fluid Mech.* **61**, 1–21.

Barthès-Biesel, D. & Acrivos, A. 1973*b* Rheology of suspensions and its relation to phenomenological theories for non-Newtonian fluid. *Int. J. Multiphase Flow* **1**, 1–24.

Bazhlekov, I. B., Anderson, P. D. & Meijer, H. E. H. 2004 Boundary integral method for deformable interfaces in the presence of insoluble surfactants. *Lect. Notes Comput. Sci.* **2907**, 355–362.

Bazhlekov, I. B., Anderson, P. D. & Meijer, H. E. H. 2006 Numerical investigation of the effect of insoluble surfactants on drop deformation and breakup in simple shear flow. *J. Coll. Intl Sci.* **298**, 369–394.

Bławzdziewicz, J., Vlahovska, P. & Loewenberg, M. 2000 Rheology of a dilute emulsion of surfactant-covered spherical drops. *Physica A* **276**, 50–80.

Booty, M. R. & Siegel, M. 2005 Steady deformation and tip-streaming of a slender bubble with surfactant in an extensional flow. *J. Fluid Mech.* **544**, 243–275.

Chaffey, C. & Brenner, H. 1967 A second-order theory for shear deformation of drops. *J. Coll. Intl Sci.* **24**, 258–269.

Cichocki, B., Felderhof, B. U. & Schmitz, R. 1988 Hydrodynamic interactions between two spherical particles. *PhysicoChem. Hyd.* **10**, 383–403.

Cox, R. G. 1969 The deformation of a drop in a general time-dependent fluid flow. *J. Fluid Mech.* **37**, 601.

Edmonds, A. R. 1960 *Angular Momentum in Quantum Mechanics*. Princeton University Press.

Eggleton, C., Tsai, T. & Stebe, K. 2001 Tip streaming from a drop in the presence of surfactants. *Phys. Rev. Lett.* **87**, 048302.

Eggleton, C. D., Pawar, Y. P. & Stebe, K. J. 1998 Insoluble surfactants on a drop in an extensional flow: a generalization of the stagnated surface limit to deforming interfaces. *J. Fluid Mech.* **385**, 79–99.

Feigl, K., Megias-Alguacil, D., Fischer, P. & Windhab, E. 2007 Simulation and experiments of droplet deformation and orientation in simple shear flow with surfactants. *Chem. Engng Sci.* **62**, 3242–3258.

Fischer, P. & Erni, P. 2007 Emulsion drops in external flow fields – the role of liquid interfaces. *Curr. Opin. Coll. Interface Sci.* **12**, 196–205.

Flumerfelt, R. W. 1980 Effects of dynamic interfacial properties on drop deformation and orientation in shear and extensional flow fields. *J. Colloid Interface Sci.* **76**, 330–349.

Frankel, N. & Acrivos, A. 1970 The constitutive equation for a dilute emulsion. *J. Fluid Mech.* **44**, 65–78.

Greco, F. 2002 Second-order theory for the deformation of a Newtonian drop in a stationary flow field. *Phys. Fluids* **14**, 946–954.

Ha, J., Yoon, Y. & Leal, L. G. 2003 The effect of compatibilizer on the coalescence of two drops in flow. *Phys. Fluids* **15**, 849–867.

Hu, Y. & Lips, A. 2003 Estimating surfactant surface coverage and decomposing its effect on drop deformation. *Phys. Rev. Lett.* **91**, 044501.

Hu, Y. T. 2008 Determination of interfacial tension between two immiscible polymers with and without surfactants at the interface. *J. Coll. Intl Sci.* **319**, 287–294.

Hu, Y. T., Pine, D. J. & Leal, L. G. 2000 Drop deformation, breakup, and coalescence with compatibilizer. *Phys. Fluids* **12**, 484–489.

Hudson, S. D., Jamieson, A. M. & Burkhart, B. E. 2003 The effect of surfactant on the efficiency of shear-induced drop coalescence. *J. Coll. Intl Sci.* **265**, 409–421.

James, A. J. & Lowengrub, J. 2004 A surfactant-conserving volume-of-fluid method for interfacial flows with insoluble surfactant. *J. Comput. Phys.* **201**, 685–722.

Jeon, H. K. & Macosko, C. W. 2003 Visualization of block copolymer distribution on a sheared drop. *Polymer* **44**, 5381–5386.

Jones, M. N. 1985 *Spherical Harmonics and Tensors for Classical Field Theory*. Wiley.

Kim, S. & Karrila, S. J. 1991 *Microhydrodynamics: Principles and Selected Applications*. Butterworth-Heinemann.

Lebedev, V. V., Turitsyn, K. S. & Vergeles, S. S. 2007 Dynamics of nearly spherical vesicles in an external flow. *Phys. Rev. Lett.* **99**, 218101.

Lee, J. & Pozrikidis, C. 2006 Effect of surfactants on the deformation of drops and bubbles in navier-stokes flow. *Comput. Fluids* **35**, 43–60.

Lequeux, F. 1998 Emulsion rheology. *Curr. Opin. Colloid Interface Sci.* **3**, 408–411.

Li, X. & Pozrikidis, C. 1997 The effect of surfactants on drop deformation and on the rheology of dilute emulsions in Stokes flow. *J. Fluid Mech.* **341**, 165–194.

Milliken, W. J., Stone, H. A. & Leal, L. G. 1993 The effect of surfactant on transient motion of Newtonian drops. *Phys. Fluids* A **5**, 69–79.

Misbah, C. 2006 Vacillating breathing and tumbling of vesicles under shear flow. *Phys. Rev. Lett.* **96**, 028104.

Muradoglu, M. & Tryggvason, G. 2008 A front-tracking method for computation of interfacial flows with soluble surfactants. *J. Comput. Phys.* **227**, 2238–2262.

Pawar, Y. & Stebe, K. J. 1996 Marangoni effects on drop deformation in an extensional flow: The role of surfactant physical chemistry. I. Insoluble surfactants. *Phys. Fluids* **8**, 1738–1751.

Pozrikidis, C. 1992 *Boundary Integral and Singularity Methods for Linearized Viscous Flow*. Cambridge University Press.

Pozrikidis, C. 2001 Numerical investigation of the effect of surfactants on the stability and rheology of emulsions and foam. *J. Engng Math.* **41**, 237–258.

Pozrikidis, C. 2004 A finite-element method for interfacial surfactant transport, with application to the flow-induced deformation of a viscous drop. *J. Engng Math.* **49**, 163–180.

Rallison, J. M. 1980 Note on the time-dependent deformation of a viscous drop which is almost spherical. *J. Fluid Mech.* **98**, 625–633.

Rallison, J. M. 1984 The deformation of small viscous drops and bubbles in shear flows. *Ann. Rev. Fluid Mech.* **16**, 45–66.

Rother, M. A. & Davis, R. H. 2004 Buoyancy driven coalescence of spherical drops covered with incompressible surfactant at arbitrary peclet number. *J. Coll. Intl Sci.* **270**, 205–220.

Rother, M. A., Zinchenko, A. Z. & Davis, R. H. 2006 Surfactant effects on buoyancy-driven viscous interactions of deformable drops. *Coll. Surf.* A **282**, 50–60.

Schowalter, W., Chaffey, C. & Brenner, H. 1968 Rheological behavior of a dilute emulsion. *J. Coll. Intl Sci.* **26**, 152–160.

Seifert, U. 1999 Fluid membranes in hydrodynamic flow fields: formalism and an application to fluctuating quasispherical vesicles. *Eur. Phys. J.* B **8**, 405–415.

Stone, H. A. 1990 A simple derivation of the time-dependent convective-diffusion equation for surfactant transport along a deforming interface. *Phys. Fluids* A **2**, 111–112.

Stone, H. A. 1994 Dynamics of drop deformation and breakup in viscous fluids. *Ann. Rev. Fluid Mech.* **26**, 65–99.

Stone, H. A. & Leal, L. G. 1990 The effects of surfactants on drop deformation and breakup. *J. Fluid Mech.* **220**, 161–186.

Taylor, G. I. 1934 The formation of emulsions in definable fields of flow. *Proc. R. Soc. Lond.* A **146**, 501–523.

Tucker, C. & Moldenaers, P. 2002 Microstructural evolution in polymer blends. *Ann. Rev. Fluid Mech.* **34**, 177–210.

Van Hemelrijck, E., Van Puyvelde, P., Velankar, S., Macosko, C. W. & Moldenaers, P. 2004 Interfacial elasticity and coalescence suppression in compatibilized polymer blends. *J. Rheol.* **48**, 143–158.

Van Puyvelde, P., Velankar, S. & Moldenaers, P. 2001 Rheology and morphology of compatibilized polymer blend. *Curr. Opin. Coll. Intl Sci.* **6**, 457–463.

Varshalovich, D. A., Moskalev, A. N. & Kheronskii, V. K. 1988 *Quantum Theory of Angular Momentum*. World Scientfic.

Velankar, S., Van Puvede, P., Mewis, J. & Moldenaers, P. 2001 Effect of compatibilization on the breakup of polymeric drops in shear flow. *J. Rheol.* **45**, 1007–1019.

Velankar, S., Van Puyvelde, P., Mewis, J. & Moldenaers, P. 2004*a* Steady shear rheological properties of model compatibilized blends. *J. Rheol.* **48**, 725–744.

Velankar, S., Zhou, H., Jeon, H. K. & Macosko, C. 2004*b* Cfd evaluation of drop retraction methods for the measurement of interfacial tension of surfactant-laden drops. *J. Coll. Intl Sci.* **272**, 172–185.

Vlahovska, P. 2003 Dynamics of a surfactant-covered drop and the non-Newtonian rheology of emulsions. PhD thesis, Yale University (pdf file available by email: petia@aya.yale.edu).

Vlahovska, P., Bławzdziewicz, J. & Loewenberg, M. 2005 Deformation of a surfatant-covered drop in a linear flow. *Phys. Fluids* **17**, Art. No. 103103.

Vlahovska, P. M. 2007 http://engineering.dartmouth.edu/∼petia_vlahovska/dropdef.html.

Vlahovska, P. M. & Gracia, R. 2007 Dynamics of a viscous vesicle in linear flows. *Phys. Rev. E* **75**, 016313.

Wong, H., Rumschitzki, D. & Maldarelli, C. 1996 On the surfactant mass balance at a deforming fluid interface. *Phys. Fluids* **8**, 3203–3204.

Xu, J. J., Li, Z. L., Lowengrub, J. & Zhao, H. K. 2006 A level-set method for interfacial flows with surfactant. *J. Comput. Phys.* **212**, 590–616.

Yon, S. & Pozrikidis, C. 1998 A finite-volume/boundary-element method for flow past interfaces in the presence of surfactants, with application to shear flow past a viscous drop. *Comput. Fluids* **27**, 879–902.